Food Research International 172 (2023) 113178

Contents lists available at ScienceDirect

Food Research International

journal homepage: www.elsevier.com/locate/foodres

A comprehensive analytical framework integrating liquid chromatography-tandem mass spectrometry metabolomics with chemometrics for metabolite profiling of lettuce varieties and discovery of antibacterial agents

Asmaa M. Otify [a,*], Shahira A. ElBanna [b], Basma M. Eltanany [c], Laura Pont [d,e], Fernando Benavente [d,*], Rana M. Ibrahim [a]

[a] Department of Pharmacognosy, Faculty of Pharmacy, Cairo University, Cairo 11562, Egypt
[b] Department of Microbiology and Immunology, Faculty of Pharmacy, Cairo University, Cairo 11562, Egypt
[c] Department of Analytical Chemistry, Faculty of Pharmacy, Cairo University, Cairo 11562, Egypt
[d] Department of Chemical Engineering and Analytical Chemistry, Institute for Research on Nutrition and Food Safety (INSA·UB), University of Barcelona, Barcelona 08028, Spain
[e] Serra Húnter Program, Generalitat de Catalunya, Barcelona 08007, Spain

ARTICLE INFO

Keywords:
Antibacterial
Antihemolytic
Chemometrics
hla transcription
LC-MS/MS
Lettuce
Metabolomics
Molecular network

ABSTRACT

This study comprehensively characterized the metabolite profiles of six lettuce varieties and established the correlation between the elucidated profiles and their antivirulence effects. A total of 195 metabolites were annotated using LC-QTOF-MS/MS metabolomics assisted by molecular networking and integrated with chemometrics. Red varieties (red *longifolia* and *lolla rosa*) demonstrated higher chlorogenic and chicoric acids suggesting their antioxidant properties. In parallel, amino acids and disaccharides were enriched in romaine *longifolia* rationalizing its palatable taste and nutritional potential, while *crispa*, *capitata*, and *lolla bionda* presented a high β-carboline alkaloid content. The antibacterial and antihemolytic potential of all varieties against methicillin-sensitive and methicillin-resistant *Staphylococcus aureus* was assessed and validated by prominent downregulation of α-hemolysin transcriptional levels in both strains. Moreover, correlation analysis revealed sesquiterpenes, β-carboline alkaloids, amino acids, and oxy-fatty acids as the main bioactives. Results emphasize lettuce significance as a functional food and nutraceutical source, and highlight varieties naturally rich in antibacterial agents to adapt breeding programs.

1. Introduction

There is an increasing interest by consumers in foods that enhance well-being, and increase the life span, in addition to meeting nutritional needs. Increased vegetable consumption has been linked to a lower risk of chronic diseases, such as cancer, age-related functional problems, and cardiovascular diseases. Macro- and micro-nutrients and bioactive compounds found in vegetables are thought to be responsible for these health benefits (Hung et al., 2004).

Lettuce (*Lactuca sativa* L.) is a widely grown and popularly consumed leafy vegetable that belongs to the family Asteraceae. Evidence from Egyptian tomb paintings revealed that it was cultivated before 4500 BCE for oil or forage. Ancient Egyptians were the first to produce the plant, which then spread to Rome and Greece, and eventually to most of

Abbreviations: ANOVA, analysis of variance; **ca**, *capitata*; **CIP**, ciprofloxacin; **cr**, *crispa*; DMSO, dimethyl sulfoxide; ESI-MS, electrospray ionization mass spectrometry; *FAO*, Food and Agriculture Organization; GNPS, global natural products social molecular networking; *L.*, *Lactuca*; **lb**, *lolla bionda*; LC-MS, liquid chromatography-mass spectrometry; **log**, *longifolia* green; **lor**, *longifolia* red; **lr**, *lolla rosa*; MRSA, methicillin-resistant *Staphylococcus aureus*; MS/MS, tandem MS; MSSA, methicillin-sensitive *Staphylococcus aureus*; OD, optical density; OPLS-DA, orthogonal partial least squares discriminant analysis; PBS, phosphate buffer saline; PLS, partial least squares; PCA, principal component analysis; qPCR, quantitative polymerase chain reaction; QTOF, quadrupole time-of-flight t_r, retention time; VIP, variable importance in the projection; ZOI, zone of inhibition.

* Corresponding authors.
E-mail addresses: asmaa.otify@pharma.cu.edu.eg (A.M. Otify), fbenavente@ub.edu (F. Benavente).

https://doi.org/10.1016/j.foodres.2023.113178
Received 1 May 2023; Received in revised form 17 June 2023; Accepted 19 June 2023
Available online 20 June 2023

Europe (Lindqvist, 1960). According to data from the statistical agency of the Food and Agriculture Organization (FAO) of the United Nations, Egypt ranked 22nd in 2021 among lettuce worldwide producers, in a ranking led by China, USA, India, and Spain (FAOSTAT Statistical Database, 2021). Lettuce occurs in a wide range of colors, shapes, and sizes, and because of this diversity, it can be classified into several varieties. A variety is a taxonomic rank below species sharing genetic and morphological similarities. The most common lettuce varieties based on leaf morphological characteristics are romaine lettuce, crispy, headed, leafy, stem, and oily (Pink & Keane, 1993). Like several major crop plants, lettuce has been subjected to intensive breeding activities to obtain genotypes with improved quality traits such as taste, health potential, and nutritional value. In terms of nutritional value, lettuce makes a minimal nutritional contribution to diet, primarily due to its high water content (~95%). However, being an extremely popular vegetable that is eaten raw, and considering its bulk consumption, it was rated 4th behind tomato, citrus, and potato in terms of the whole nutritional diet contents (Kenny & O'Beirne, 2009; Pink & Keane, 1993). With such popularity worldwide, it is important to understand and compare the composition of lettuce varieties, in order to identify those delivering the most health-promoting bioactive compounds.

Metabolomics is described as the comprehensive analysis of the complete set of small molecules or metabolites (*i.e.*, the metabolome) within a certain biological sample, including vegetables with edible greens, such as lettuce. Metabolomics frequently involves untargeted analyses with hyphenated mass spectrometry (MS) techniques, such as liquid chromatography electrospray ionization mass spectrometry (LC-ESI-MS), followed by multivariate data analysis with advanced chemometrics methods. Mass spectrometers with quadrupole time-of-flight (QTOF) analyzers are typically used for untargeted metabolomics analyses because they have a very high scan rate and can acquire MS and tandem MS (MS/MS) spectra with high mass accuracy and resolution (Köfeler et al., 2012). Thereby, different authors have shown the successful application of LC-ESI-QTOF-MS/MS metabolomics and chemometrics for the quality control of food products, *e.g.*, tomato and *Pinus* (Otify et al., 2023; Saber et al., 2021). Furthermore, the use of molecular networking *via* the global natural products social molecular networking (GNPS) platform for the visual inspection of MS/MS spectra has recently increased, assisting metabolite identification and observation of their relative abundance in the analyzed samples (Otify et al., 2023).

Antimicrobial resistance constitutes a major health problem in the 21st century. Different studies have been directed toward recruiting new therapeutic strategies (Prestinaci et al., 2015). Antivirulence therapy is a recent approach that can provide effective control of disease severity with virulence inhibitors rather than with bactericides. *Staphylococcus aureus* is a challenging gram-positive bacterium that poses a high risk of developing antibiotic resistance over time. Indeed, it is the common cause of some serious infections such as endocarditis, skin or soft tissue, bone, and joint infections, which may progress into bacteremia and septicemia (Tong et al., 2015). In particular, methicillin-resistant *S. aureus* (MRSA) strains are superbugs that account for most staphylococcal infections, causing severe morbidity and mortality that need to be reduced (Cosgrove et al., 2003). Potential antivirulence agents are currently being developed to affect different targets, *e.g.*, disassembly of bacterial functional membrane microdomains, disruption of biofilm formation, and bacterial toxin neutralization (Fleitas Martínez et al., 2019). Hemolysins are toxins that help bacteria to disrupt cell membranes during infection (Dinges et al., 2000). Alpha-hemolysin, encoded by the *hla* gene, is one of the most prevalent virulence factors produced by ~ 95% of *S. aureus* strains and it is highly correlated with disease severity during infections (Grumann et al., 2014).

The main goal of this study is the development of a non-targeted LC-ESI-QTOF-MS and MS/MS method combined with molecular networking and multivariate data analysis applicable to the comprehensive characterization of lettuce metabolites to provide insight into the chemotaxonomic relatedness among 6 different varieties, namely, *capitata* (batavia or crisphead lettuce, **ca**); *longifolia* (romaine lettuce, red (**lor**) and green (**log**)); *crispa* (oakleaf lettuce, **cr**); *lolla rossa* (red coral lettuce, **lr**); and *lolla bionda* (green coral lettuce, **lb**). The combination of LC-MS/MS and chemometrics offers a valuable tool for comparing the metabolite profiles of the different lettuce varieties, as well as for identifying those primary and secondary metabolites correlated with the antibacterial or antivirulence activities against MRSA or methicillin-sensitive *S. aureus* (MSSA). This comprehensive LC-MS/MS metabolite profiling, comparison, and bioactivity assessment against non-antibiotic and antibiotic resistant bacteria of six lettuce varieties represents a great advancement, as previous LC-MS studies on lettuce metabolites have been directed to characterize specific compounds, such as polyphenols (Pepe et al., 2015), vitamins and carotenoids (Kim et al., 2016), or di- and triglycerides (Byrdwell et al., 2021) or focused on a specific variety (Ismail et al., 2019; Pepe et al., 2015). The described strategy allows for revealing the lettuce varieties with the greatest bioactivity potential and the metabolites responsible for such functionality, which may be considered to adapt future breeding programs.

2. Experimental

2.1. Plant material

Leaves of 6 *L. sativa* green and red varieties, namely, **ca**, **cr**, **lb**, and **log** (green) and **lor** and **lr** (red), were collected from Makar Farms (Cairo, Egypt) in December 2020. The plant material was authenticated by staff members of the Flora and Phytotaxonomy Research Department (Horticulture Research Institute, Egypt). Voucher specimens (03032021 I-V) were deposited at the herbarium of the Pharmacognosy Department (Faculty of Pharmacy, Cairo University, Egypt). Suppl. Table (S1) displays the morphological characteristics of the 6 lettuce varieties evaluated in this study. The selected leaves represent a wide range of shapes and colors found in commercial lettuces, *e.g.*, green and red colored types, rounded and long leaves, etc.

2.2. Preparation of plant extracts

Lettuce leaves were shade-dried at room temperature (not exceeding 25 °C) and protected from direct sunlight to avoid the degradation of labile constituents (Thamkaew et al., 2021). The leaves were then powdered with a powder grinder machine, and the powdered plant material (60 g each) was extracted twice using 1 L of methanol (analytical grade, El-Gomhuria Company, Cairo, Egypt) at 25 °C. Solvent extracts were filtered, and the filtrates were evaporated at 50 °C until dryness in a rotary evaporator. For LC-MS/MS analysis, samples were prepared by dissolving 10 mg of each extract in 1 mL of methanol, centrifuging at 13,000 x g for 10 min, and filtering through a 0.22 μm syringe nylon filter. For each lettuce sample, 3 biological replicates were prepared and extracted in parallel under the same conditions.

2.3. LC-MS/MS metabolite profiling

Mass spectra were acquired in the negative mode following the protocol of (Ibrahim et al., 2023). LC-MS/MS analyses were done on a 1260 Infinity liquid chromatograph coupled to a 6546 LC-QTOF mass spectrometer equipped with an orthogonal ESI interface (Agilent Technologies, Waldbronn, Germany). All solvents used were of LC-MS grade (Merck, Darmstadt, Germany). Chromatographic separations were performed at room temperature and 350 μL/min flow rate using a Zorbax SB-C18 column (2.1 mm × 150 mm, pore diameter 90 Å, particle size 5 μm, Agilent Technologies). Mobile phase solvents were (A) water and (B) acetonitrile (both with 0.1% (v/v) formic acid) and were degassed by sonication before use (10 min). The gradient (%B (v/v)) for separation and re-equilibration was: isocratic 5% (0–1 min) and linear from 5% to 95% (1–16 min), then isocratic 95% (16–18 min), linear from 95% to 5% (18–20 min), and finally isocratic 5% (20–25 min). The sample injection

volume was 5 μL with the autosampler at 4 ℃. The following parameters were used to run the QTOF mass spectrometer in negative ESI mode: capillary voltage 3500 V, nebulizer gas 30 psi, fragmentor voltage 150 V, drying gas flow rate 8 L/min, drying gas temperature, 350 ℃, skimmer voltage 60 V, and OCT 1 RF Vpp voltage 300 V. The MS and MS/MS scan rates were 10 spectra/s and a 6 spectra/s, respectively, and the auto-MS/MS mode was employed over the 50–2000 *m/z* range. The MassHunter software (B.06.01 Service Pack1, Agilent Technologies) was used for instrument control, data acquisition, and processing of the MS/MS spectra. Detected compounds were characterized by their retention time (t_r), accurate molecular monoisotopic mass, and MS/MS spectra. Metabolites were annotated by comparing with free databases, such as the Human Metabolome Database (http://www.hmdb.ca/), the Phytochemical Dictionary of Natural Product Database (https://dnp.chemnetbase.com/faces/chemical/ChemicalSearch.xhtml), MassBank of North America (https://mona.fiehnlab.ucdavis.edu/), ReSpect Library (Sawada et al., 2012), and LipidMaps (https://www.lipidmaps.org/), as well as with additional literature.

2.4. Molecular networking

Metabolite annotations were further confirmed by molecular networking. The mzXML files were uploaded using WinSCP (https://winscp.net) into the GNPS online platform (https://gnps.ucsd.edu) to generate a molecular network. The parameters used for creating the network *via* GNPS and the established molecular network can be accessed *via* the following link: https://gnps.ucsd.edu/ProteoSAFe/status.jsp?task=96df6f7bbce44754a8b5068b71d20003. Cytoscape 3.9.1 (https://cytoscape.org) was used for molecular network visualization. Therefore, the annotated metabolites were identified at a high confidence level, *i.e.*, level 2: probable structure with library/ bibliography spectral data match (Schymanski et al., 2014).

2.5. Bioactivity evaluation

2.5.1. Bacterial strains

MSSA ATCC 6538 and MRSA USA300 strains were used to assess the antibacterial and antivirulence activities of lettuce samples.

2.5.2. Determination of antibacterial activity

The agar-well diffusion method was applied to assess the antibacterial activity of lettuce extracts (Gonelimali et al., 2018). MSSA and MRSA strains were cultured in Mueller-Hinton broth (Difco, USA), and incubated for 20 h at 37℃ with shaking at 180 rpm. The optical density (OD) of the overnight bacterial suspensions was measured at 600 nm and adjusted by dilution to 0.08–0.1 (equal to 0.5 MacFarland standard, ~1.5×10^8 CFU/mL). Then, Mueller-Hinton agar plates were subjected to surface inoculation using cotton swabs loaded with the diluted cultures of both bacteria, followed by perforation using a sterile cork pourer (10–11 mm diameter).

For each lettuce extract, a working solution of 1.5 mg/μL in dimethyl-sulfoxide (DMSO, Sigma-Aldrich, Germany) was prepared. Then, 150 μL of each extract was added to the wells of the inoculated agar plates (225 mg extract/well). Besides, 100 μL of ciprofloxacin (CIP, 50 μg/mL, Amriya Pharm, Egypt) was used as a reference (5 μg CIP/well) (Weinstein, 2018) and 150 μL of pure DMSO as a negative control. The diameters of the zones of inhibition (ZOI) of the extracts, if present, were recorded and statistically compared to the ZOI of DMSO.

2.5.3. Determination of the antihemolytic effect

The ability of the lettuce extracts to affect hemolysins secretion of both *S. aureus* strains was evaluated using a hemolytic assay after overnight incubation with or without the extracts (Feng et al., 2021). Briefly, overnight cultures were diluted in tryptic soya broth (Difco, USA) to an OD at 600 nm of ~ 0.1. The diluted cultures were then incubated with or without different sub-inhibitory concentrations of the extracts, to a final concentration of 12.5 mg/mL at 37 ℃ with shaking at 180 rpm for 20 h. The bacterial cultures growth was estimated by measuring the OD at 600 nm, followed by centrifugation and collection of the supernatants to test the hemolytic activity. The hemolytic assay was conducted by mixing equal volumes of the supernatants with 4% rabbit blood cells, followed by incubation at 37 ℃ in a water bath for 45 min (the used protocol was approved by the Research Ethics Committee of the Faculty of Pharmacy, Cairo University, approval code: MI(3127)). Simultaneously, different blanks were prepared by mixing equal volumes of tryptic soya broth supplemented with each extract and 4% rabbit blood cells. In addition, 1% Triton X-100 and sterile phosphate buffer saline (PBS) were included as positive and negative hemolytic references, respectively. Subsequently, centrifugation at 22,000 x g for 5 min was applied to all blood cell-*S. aureus* supernatants and controls before determining the hemolytic activity by measuring the absorbance of the recovered supernatants at 540 nm. To overcome variations caused by differences in growth, the actual hemolysis was determined as the ratio between the absorbance at 540 nm and the OD at 600 nm.

Then, the percentage of hemolytic activity of both strains that grew in the presence or absence of such extracts was calculated relative to Triton X-100 (a positive hemolytic control). Finally, the antihemolytic effect of the tested extracts was estimated by calculating the percentage of inhibition in the hemolytic activity as follows:

$$\frac{\text{Hemolysis \% of } S.\ aureus \text{ (DMSO)} - \text{Hemolysis \% of } S.\ aureus \text{ with extract}}{\text{Hemolysis \% of } S.\ aureus \text{ (DMSO)}} \times 100$$

2.5.4. Transcriptional analysis of hla gene

Both MSSA and MRSA strains were grown to late exponential phase under the effect of selected lettuce extracts (**log**, **lor**, **ca**, and **cr**). For each culture extract case, cells were harvested, and RNA extraction was performed using RNeasy Mini kit (Qiagen, Germany) followed by DNase treatment using RQ1 RNase-Free DNase I enzyme (Promega, USA) to avoid any possible DNA carryover. cDNA was synthesized by GoScript™ Reverse Transcription System (Promega, USA) for evaluation of the *hla* transcriptional levels of the corresponding cultures. Finally, quantitative polymerase chain reaction (qPCR) analysis was conducted in a Rotor-Gene-Q real-time PCR instrument (Qiagen, Germany) using the synthesized cDNAs and SensiFAST™ SYBR Lo-ROX Kit (Bioline, UK) according to the manufacturer's instructions. The *hla* primers and 16S rRNA housekeeping genes for the quantification are shown in Suppl. Table (S2). The relative quantification of the *hla* transcriptional level was estimated using the ΔΔCt method with the Rotor-Gene-Q software (Livak & Schmittgen, 2001). The results were expressed as a fold change in the *hla* message for cultures exposed to the studied lettuce extracts relative to those exposed to DMSO only (calibrator).

2.5.5. Statistical analysis

Analysis of variance (ANOVA), followed by *post-hoc* multiple *t*-tests, with Tukey correction were applied on the antibacterial and antihemolytic assays with GraphPad Prism 5 (GraphPad Software, USA).

2.6. Multivariate data analysis

2.6.1. Data preprocessing

MassHunter raw LC-MS chromatograms were converted into mzXML format with MSConvert 3.0 software (https://www.proteowizard.org). The converted data files were then imported to metAlign software (https://doi.org/10.5281/zenodo.7273832) with the following baseline and noise elimination parameters: 1–10^5 scan number, 10^7 maximum peak amplitude, peak slope = 1.0, peak threshold factor = 2, and average peak width at half height = 5. The peak lists were all aligned with no scaling or pre-alignment processing. MetAlign output dataset was then converted into a CSV file, providing a data matrix with

information from all samples (extracts of 6 lettuce varieties analyzed in triplicate), where columns were the scan number, t_r, mass-to-charge ratio (*m/z*), and peak intensity for the detected compounds. Compounds below 100 *m/z* were excluded from the final data matrix consisting of 18 columns (sample extracts) × 838 rows (peak intensity for each detected compound). The dataset was mean-centered, exported to SIMCA-P (version 14, Umetrics, Umeå, Sweden), and Pareto scaled before multivariate data analysis.

2.6.2. Multivariate data analysis

Variations among lettuce varieties were investigated by unsupervised and supervised multivariate data analysis methods, namely principal component analysis (PCA) and orthogonal partial least squares-discriminant analysis (OPLS-DA). PCA on the LC-MS dataset was performed considering (i) the whole run time (t_r 0–24 min) and (ii) the early time region (t_r 0–10.76 min) to mainly focus on secondary metabolites.

The correlation between the bioactivities and the LC-MS dataset of the annotated metabolites was achieved by performing partial least squares (PLS) analysis. Then, the variable importance in the projection (VIP) values from the PLS analysis were used to identify the main contributing metabolites to the bioactivities. The correlation analysis was further expanded by calculating Pearson's correlation coefficient (r), and a correlogram was created to illustrate the strength of the relationship among metabolites and bioactivities. The correlogram plot was done using RStudio (version 2022.07.1, Boston, MA, USA), and the following threshold values were used to determine the correlation: $r < 0.3$, negligible correlation; $r = 0.3–0.5$, weak correlation; $r = 0.5–0.7$, moderate correlation; $r = 0.7–0.9$, strong correlation; and $r = 0.9–1.0$, very strong correlation (Mukaka, 2012).

PLS and OPLS-DA models were validated by permutation tests ($n = 200$) and regression analysis. The model fitness parameters (goodness of fit: R^2_Y; goodness of prediction: Q^2_Y; and cross-validation: CV-ANOVA, $p < 0.01$) were also determined.

3. Results and discussion

3.1. LC-MS/MS metabolite profiling assisted by molecular networking

Representative base peak chromatograms of *L. sativa* extracts obtained by LC-MS in negative ESI mode for the different varieties are depicted in Suppl. Fig. (S1) and MS/MS spectra of some of the most relevant annotated metabolites are shown in Suppl. Fig. (S2-S24). The negative ESI mode was preferred because it allowed better sensitivity for a wide range of the expected metabolite classes, *e.g.*, organic acids, amino acids, and phenolic compounds, compared to the positive ESI mode (Ibrahim et al., 2023; Liigand et al., 2017). A total of 195 metabolites, summarized in Table 1 and Fig. 1, were tentatively identified considering the measured accurate molecular mass and MS/MS spectra, by comparing with free databases and additional literature. The annotated metabolites belonged to a vast array of classes, *i.e.*, sugars, organic acids, amino acids, alkaloids, nucleosides, phenolic acids, flavonoids, sesquiterpenes, fatty acids, and lipids.

Metabolite annotations were further confirmed by molecular networking. Molecular networking is based on the fact that structurally similar metabolites have comparable MS/MS fragmentation patterns, enabling the visual investigation of metabolite families (clusters) (Otify et al., 2023). Within the established network (Suppl. Fig. S25), each node corresponds to one MS/MS spectrum and is labeled with its molecular ion *m/z* value. Nodes were represented by pie charts and colored according to the sample types to reflect their relative abundance in the 6 lettuce varieties. Those nodes having similar fragmentation patterns were connected with lines (edges), which indicate the mass differences between these nodes (Suppl. Fig. S25). The constructed molecular network is composed of 253 nodes, 493 edges, and presented 17 clusters (a minimum of 2 connected nodes). The clusters of interest were **A & B** (lipids), **C & F** (fatty acids), **D** (amino acids), **E** (alkaloids), and **G** (phenolic acids).

To the best of our knowledge, this is the first comprehensive metabolite profiling of 6 varieties of *L. sativa*, coupled with molecular network and chemometrics, which is intended to provide chemical-based evidence for their differential biological effect on antibiotic resistant bacteria. Chemometric tools allowed unbiased sample discrimination, whereas GNPS enabled the detailed analysis of tandem mass data. The following paragraphs detail the structural elucidation of the annotated metabolites.

3.1.1. Amino acids

LC-MS/MS spectral analysis indicated that nearly all examined lettuce samples encompassed similar amino acids (Table 1) including hexosyl asparagine (**9**) [*m/z* 293.0996 ($C_{10}H_{17}N_2O_8$)$^-$], hexosyl valine (**16**) [*m/z* 278.1248 ($C_{11}H_{20}NO_7$)$^-$], hexosyl pyroglutamic acid (**17**) [*m/z* 290.0886 ($C_{11}H_{16}NO_8$)$^-$], and hexosyl phenylalanine (**28**) [*m/z* 326.1248 ($C_{15}H_{20}NO_7$)$^-$]. These amino acids showed the same fragmentation behavior, which is loss of the attached sugar unit and formation of a base peak [M−162]$^-$ at *m/z* 131, 116, 128, and 164 in metabolites **9**, **16**, **17**, and **28**, respectively (Suppl. Fig. S2). Interestingly, molecular networking unveiled the presence of an amino acid cluster of 3 nodes (cluster D) including hexosyl pyroglutamic acid (**17**), hexosyl isoleucine (**23**), and hexosyl phenyl alanine (**28**) (Suppl. Fig. S25).

3.1.2. Alkaloids

Three alkaloids were detected in the investigated samples, namely, tetrahydro-β-carboline-carboxylic acid (**50**) [*m/z* 215.0830 ($C_{12}H_{11}N_2O_2$)$^-$], tetrahydro-β-carboline (**52**) [*m/z* 171.0930 ($C_{11}H_{11}N_2$)$^-$], and tetrahydro-β-carboline-dicarboxylic acid (**53**) [*m/z* 259.0726 ($C_{13}H_{11}N_2O_4$)$^-$] (Choi et al., 1988). All alkaloids showed an intense ion at *m/z* 171 corresponding to the tetrahydro-β-carboline moiety and other ions at *m/z* 142, 129, and 116 due to *retro*-Diels Alder fissure (Table 1 & Suppl. Fig. S3). β-Carboline alkaloids have wide distributions among vegetables and fruits and have been reported in *L. sativa* (Ismail et al., 2019). Cluster E (Suppl. Fig. S25) revealed the presence of 2 alkaloids, namely, tetrahydro-β-carboline-carboxylic acid (**50**) and tetrahydro-β-carboline-dicarboxylic acid (**53**).

3.1.3. Organic acids

Five organic acids were detected and their fragmentation behavior showed characteristic losses of CO_2 [M−44]$^-$ and H_2O [M−18]$^-$ (Table 1). In detail, peak **15** [*m/z* 133.0143 ($C_4H_5O_5$)$^-$] showed a base peak at *m/z* 71 resulting from the successive losses of CO_2 and H_2O [M−44−18]$^-$ and was annotated as malic acid (Suppl. Fig. S4). Similarly, the spectrum of peak **20** [*m/z* 191.0197 ($C_6H_7O_7$)$^-$] revealed an intense ion at *m/z* 111 due to the successive losses of CO_2 and $2H_2O$ [M−44−2*18]$^-$ and was characterized as citric acid (Suppl. Fig. S4). According to recent studies, the high abundance of organic acids provides carbon building blocks for producing defensive compounds in plants that function as phytoalexins during the sprouting stage (Schwachtje et al., 2018). Moreover, organic acids are important components of foodstuff, highly contributing to organoleptic characteristics as well as quality and safety (Farag et al., 2019).

3.1.4. Chlorogenic and phenolic acids

A total of 32 phenolic acids, mainly as benzoic and chlorogenic acid derivatives, were early eluted in the first part of the chromatogram (t_r 2–14 min) (Fig. 1 & Table 1).

Five chlorogenic acids were detected and characterized, namely, 1 coumaroyl quinic acid (**57**), 3 caffeoyl quinic acid isomers (**40**, **48**, & **75**), and 1 dicaffeoyl quinic acid (**76**). These assignments agreed with the reported literature (Clifford et al., 2003). 4-Caffeoyl quinic acid (**48**) [*m/z* 353.0877 ($C_{16}H_{17}O_9$)$^-$] was readily characterized by its base peak at *m/z* 173 corresponding to dehydrated quinic acid, while 5- and 3-caffeoyl quinic acids (**75** [*m/z* 353.0883 ($C_{16}H_{17}O_9$)$^-$] and **40** [*m/z*

Table 1
Metabolites tentatively identified in the methanol extracts of *L. sativa* by LC-MS/MS in negative ESI mode.

#	t_r (min)	Molecular ion *m/z*	Molecular ion formula $[M-H]^-$	Error (ppm)	MS/MS fragments	Metabolite	lor	log	cr	ca	lr	lb
Sugars/Sugar acids/Sugar alcohols												
1	0.89	317.0544	$C_9H_{17}O_{10}S^-$	1.26	225, 165, 149, 101, 81	Sulfohexosyl glycerol	–	+	+	+	+	+
3	0.93	340.1239	$C_{12}H_{22}NO_{10}^-$	1.95	142, 86, 73	Disaccharide amine	+	+	–	–	–	–
4	0.97	165.0407	$C_5H_9O_6^-$	−0.81	105, 75, 59	Pentose sugar acid	+	+	–	–	+	–
5	0.99	191.0561	$C_7H_{11}O_6^-$	0.05	109, 93, 85	Monosaccharide (Anhydroheptose)	+	+	+	+	+	+
6	1.00	135.0298	$C_4H_7O_5^-$	0.69	100, 75, 70, 52	Threonic acid	+	+	+	–	+	+
7	1.02	149.0452	$C_5H_9O_5^-$	2.48	135, 73	Monosaccharide (Pentose)	–	–	+	+	+	+
8	1.02	179.0560	$C_6H_{11}O_6^-$	−0.07	75, 71, 59	Hexose	+	–	–	–	+	–
10	1.06	195.0511	$C_6H_{11}O_7^-$	−0.49	129, 75, 71, 59	Gluconic acid	+	+	+	+	+	+
11	1.07	341.1069	$C_{12}H_{21}O_{11}^-$	7.63	89, 71, 59	Disaccharide	+	+	–	+	–	+
12	1.10	209.0666	$C_7H_{13}O_7^-$	−0.22	85	Monosaccharide (Heptose)	+	+	+	+	+	+
13	1.11	105.0193	$C_3H_5O_4^-$	−0.01	75, 59, 57	Glyceric acid	+	+	+	+	+	+
22	1.59	161.0455	$C_6H_9O_5^-$	0.23	71, 59	Monosaccharide	+	+	–	–	+	+
30	2.83	323.1338	$C_{13}H_{23}O_9^-$	3.09	279, 239, 229, 88, 79	Disaccharide (2 Deoxyhexoses + methyl)	–	–	+	–	+	+
Amino acids												
9	1.04	293.0996	$C_{10}H_{17}N_2O_8^-$	13.53	131, 114, 113	Hexosyl asparagine	+	+	+	+	+	+
14	1.16	632.2036	$C_{23}H_{38}NO_{19}^-$	0.71	200, 128	Pyroglutamic acid derivative	–	+	–	–	–	–
16	1.41	278.1248	$C_{11}H_{20}NO_7^-$	−0.39	116	Hexosyl valine	+	+	+	+	+	+
17	1.44	290.0886	$C_{11}H_{16}NO_8^-$	−1.05	200, 128	Hexosyl pyroglutamic acid	+	+	+	+	+	+
18	1.46	128.0354	$C_5H_6NO_3^-$	−0.8	128	Pyroglutamic acid	+	–	–	+	+	–
19	1.48	200.0561	$C_8H_{10}NO_5^-$	1.25	128	Pyroglutamic acid derivative	+	+	+	+	+	+
21	1.54	372.1045	$C_{12}H_{23}NO_{10}P^-$	5.49	128	Pyroglutamic acid derivative	+	+	+	+	+	+
23	1.64	292.1402	$C_{12}H_{22}NO_7^-$	−0.09	130, 101	Hexosyl isoleucine	+	+	+	+	+	+
24	1.67	202.1085	$C_9H_{16}NO_4^-$	−0.38	130	Isoleucine derivative	+	+	+	+	+	+
25	1.80	130.0872	$C_6H_{12}NO_2^-$	1.81	130, 112, 88, 84, 66, 54	Isoleucine	–	–	–	+	–	–
28	2.30	326.1248	$C_{15}H_{20}NO_7^-$	−0.86	164, 147	Hexosyl phenylalanine	–	+	+	+	+	+
29	2.62	164.0719	$C_9H_{10}NO_2^-$	−0.97	147, 103, 72	Phenylalanine	–	–	+	+	+	–
31	3.09	290.0876	$C_{11}H_{16}NO_8^-$	1.77	208, 200, 192, 128, 90, 74	Hexosyl pyroglutamic acid	–	+	–	–	–	+
34	3.91	278.1238	$C_{11}H_{20}NO_7^-$	2.57	116	Hexosyl valine	+	+	–	–	–	–
55	7.52	210.0773	$C_{10}H_{12}NO_4^-$	−1.36	124, 94	Methyldopa	+	+	+	+	+	–
84	9.92	949.6717	$C_{12}H_{21}N_2O_2^-$	−0.46	903, 677, 451, 225	Isoleucyl-isoleucine derivative ***	–	+	+	+	+	+
95	10.69	307.0725	$C_{17}H_{11}N_2O_4^-$	−0.45	263, 233, 205	Unknown amino acid	+	+	+	–	+	–
Alkaloids												
50	7.25	215.0830	$C_{12}H_{11}N_2O_2^-$	−1.97	171, 169, 156, 142, 129, 116, 92, 86	Tetrahydro-β-carboline-carboxylic acid	+	+	+	+	+	+
52	7.39	171.0930	$C_{11}H_{11}N_2^-$	−1.15	156, 144, 142, 130, 116, 92	Tetrahydro-β-carboline	+	–	–	+	–	+
53	7.47	259.0726	$C_{13}H_{11}N_2O_4^-$	−0.04	171, 142, 116, 92, 86	Tetrahydro-β-carboline-dicarboxylic acid	+	–	–	+	+	–
Nucleosides												
26	1.91	282.0844	$C_{10}H_{12}N_5O_5^-$	−4.63	150, 133	Guanosine	+	–	–	–	+	+
35	4.20	134.0470	$C_5H_6N_5^-$	1.42	108	Adenine	–	+	+	–	+	–
Organic acids												
15	1.16	133.0143	$C_4H_5O_5^-$	−0.66	115, 71	Malic acid	+	+	+	+	+	+
20	1.50	191.0197	$C_6H_7O_7^-$	0.18	129, 147, 111, 87, 85	Citric acid	+	+	+	+	+	+
43	6.25	175.0611	$C_7H_{11}O_5^-$	0.33	157, 115, 131, 113, 85	Isopropyl malic acid	+	+	+	+	+	+
61	8.11	439.1816	$C_{18}H_{31}O_{12}^-$	1.81	261, 101, 89, 73, 71, 59	Dihexosyl caproate	+	+	+	+	+	+
70	8.72	271.1552	$C_{14}H_{23}O_5^-$	−1.05	155, 59	Unknown organic acid	+	+	+	+	+	+
Chlorogenic and phenolic acids												
27	1.95	315.0734	$C_{13}H_{15}O_9^-$	−3.84	153, 152, 108	Dihydroxy benzoic acid hexoside	–	–	+	–	–	–
32	3.17	329.0876	$C_{14}H_{17}O_9^-$	2.45	167, 152, 123, 108	Hydroxy methoxy benzoic acid hexoside	–	+	+	+	+	+
33	3.27	151.0388	$C_8H_7O_3^-$	8.58	139, 137, 129, 119, 109, 107, 102	Methoxy benzoic acid	–	+	+	–	–	–
36	4.51	153.0190	$C_7H_5O_4^-$	2.33	109, 108	Dihydroxy benzoic acid	+	+	+	+	+	+
38	4.81	329.0874	$C_{14}H_{17}O_9^-$	3.64	167, 152, 123, 108	Hydroxy methoxy benzoic acid hexoside	+	–	–	–	–	–
39	5.59	179.0350	$C_9H_7O_4^-$	−0.17	141, 135, 134	Dihydroxy cinnamic acid	–	+	+	+	–	+
40	6.00	353.0873	$C_{16}H_{17}O_9^-$	1.64	191, 179, 135	3-Caffeoyl quinic acid (Chlorogenic acid)	+	+	+	–	–	–
41	6.01	359.0982	$C_{15}H_{19}O_{10}^-$	1.72	197, 182, 153, 138	Hydroxy dimethoxy benzoic acid hexoside	+	–	+	–	–	+
42	6.17	311.0404	$C_{13}H_{11}O_9^-$	1.5	179, 149, 135	Caffeoyl tartaric acid	+	+	–	+	–	–
45	6.77	343.1005	$C_{15}H_{19}O_9^-$	9.37	246, 202, 181, 146, 135, 109	Dimethoxy benzoic acid hexoside	–	+	–	–	+	–
46	6.87	163.0406	$C_9H_7O_3^-$	−4.42	119	Coumaric acid	+	+	–	–	+	+
47	7.03	485.1668	$C_{22}H_{29}O_{12}^-$	−1.32	441, 215, 197, 89, 59	Unknown phenolic acid	+	+	+	+	+	+
48	7.09	353.0877	$C_{16}H_{17}O_9^-$	−0.19	191, 173, 135	4-Caffeoyl quinic acid (Chlorogenic acid)	+	+	+	+	+	+
49	7.10	191.0562	$C_7H_{11}O_6^-$	−0.15	191, 93, 85	Quinic acid	+	+	+	+	+	+

(*continued on next page*)

Table 1 (*continued*)

#	t_r (min)	Molecular ion *m/z*	Molecular ion formula [M−H]$^-$	Error (ppm)	MS/MS fragments	Metabolite	lor	log	cr	ca	lr	lb
54	7.49	179.0351	$C_9H_7O_4^-$	−0.65	135, 134	Dihydroxy cinnamic acid	–	+	+	+	–	+
57	7.80	337.0931	$C_{16}H_{17}O_8^-$	−0.32	191, 173, 163, 93	3-Coumaroyl quinic acid (Chlorogenic acid)	+	+	+	+	+	+
56	7.59	135.0452	$C_8H_7O_2^-$	−0.62	135, 134, 117, 107	Phenylacetic acid	+	–	–	–	+	+
58	7.86	121.0299	$C_7H_5O_2^-$	−3.53	121, 92	Benzoic acid	+	–	–	+	–	+
64	8.48	167.0349	$C_8H_7O_4^-$	0.93	152, 108	Dihydroxy methyl benzoate	+	–	–	+	+	–
65	8.57	163.0405	$C_9H_7O_3^-$	−4.51	119	Coumaric acid	+	+	–	+	–	+
71	8.73	179.0343	$C_9H_7O_4^-$		135, 134	Dihydroxy cinnamic acid	–	+	+	+	–	–
72	8.75	473.0724	$C_{22}H_{17}O_{12}^-$	0.36	179, 149, 135	Dicaffeoyl tartaric acid (Chicoric acid)	+	+	+	–	+	+
73	8.86	579.2080	$C_{28}H_{35}O_{13}^-$	1.49	417, 402, 387, 181, 166, 152	Dihydroxy benzoic acid hexoside derivative	+	+	+	+	+	+
74	8.90	435.0925	$C_{20}H_{19}O_{11}^-$	1.41	315, 153, 152, 137, 109, 108, 93	Dihydroxy benzoyl hydroxybenzoyl hexoside	+	+	+	–	+	+
75	9.18	353.0883	$C_{16}H_{17}O_9^-$	−2.47	191, 173, 135, 111	5-Caffeoyl quinic acid (Chlorogenic acid)	+	+	+	+	–	–
76	9.22	515.1194	$C_{25}H_{23}O_{12}^-$	0.39	353, 191, 179, 173, 135	3,4-Dicaffeoyl quinic acid (Chlorogenic acid)	+	+	+	+	+	+
81	9.76	399.1294	$C_{18}H_{23}O_{10}^-$	0.86	153, 152, 109, 108	Dihydroxy benzoic acid derivative	+	+	–	–	+	+
83	9.87	193.0508	$C_{10}H_9O_4^-$	−0.84	161, 134, 133	Ferulic acid	+	+	+	+	+	+
89	10.21	435.0928	$C_{20}H_{19}O_{11}^-$	0.98	315, 153, 152, 137, 109, 108, 93	Dihydroxy benzoyl hydroxybenzoyl hexoside	+	+	+	+	+	–
91	10.43	423.1659	$C_{21}H_{27}O_9^-$	−2.75	179, 161	Caffeic acid derivative	+	+	+	+	+	+
94	10.56	519.1127	$C_{24}H_{23}O_{13}^-$	3.07	357, 339, 113, 69	Dibenzoyl tartaric acid hexoside	+	–	–	–	–	+
121	13.62	593.1303	$C_{30}H_{25}O_{13}^-$	0.55	209, 165, 121	Benzoic acid derivative	–	+	+	+	+	+
Flavonoids												
59	7.89	269.0476	$C_{15}H_9O_5^-$	−7.6	225, 196, 195, 183	Apigenin	+	–	–	+	–	+
67	8.63	447.0930	$C_{21}H_{19}O_{11}^-$	1.4	285, 284	Kaempferol 3-hexoside	+	+	+	+	+	+
68	8.66	463.0883	$C_{21}H_{19}O_{12}^-$	−0.16	301, 300, 271, 255, 179, 151	Quercetin 3-hexoside	+	+	–	–	+	–
69	8.69	461.0727	$C_{21}H_{17}O_{12}^-$	0.27	285, 151	Kaempferol hexuronide	+	+	–	–	+	+
92	10.53	285.0402	$C_{15}H_9O_6^-$	0.75	285, 241, 217, 199, 175, 151, 133	Luteolin	+	–	–	–	+	–
93	10.54	301.0353	$C_{15}H_9O_7^-$	1.19	179, 151	Quercetin	+	–	–	–	+	–
Other phenolics												
37	4.79	109.0291	$C_6H_5O_2^-$	7.57	109, 108, 81	Dihydroxy benzene	+	+	–	–	+	+
44	6.63	177.0210	$C_9H_5O_4^-$	−9.1	133, 105, 79	Esculetin	+	+	–	–	+	+
Sesquiterpenes												
51	7.36	454.1164	$C_{20}H_{24}NO_9S^-$	1.74	339, 172, 114, 97	15-Deoxylactucin-8-sulfate-proline	+	+	+	–	+	+
63	8.30	341.0705	$C_{15}H_{17}O_7S^-$	−0.89	97, 80	8-Deacetylmatricarin-8-sulfate	+	+	+	+	+	+
Fatty acids												
60	8.06	189.0769	$C_8H_{13}O_5^-$	−0.15	145, 129, 127, 99	Hydroxy octanedioic acid	+	+	+	+	+	+
62	8.22	307.1401	$C_{13}H_{23}O_8^-$	−0.84	307, 145, 127, 101, 81, 71, 59	Hydroxy heptanoic acid hexoside	+	+	+	+	+	+
66	8.62	391.1972	$C_{18}H_{31}O_9^-$	0.27	113, 101, 89, 71, 59	Hydroxy oxo-dodecanoic acid hexoside	+	+	–	–	–	+
77	9.29	273.1706	$C_{14}H_{25}O_5^-$	0.31	155, 111, 99, 59	Hydroxy tetradecanedioic acid	+	+	+	+	+	+
78	9.44	243.1240	$C_{12}H_{19}O_5^-$	−0.66	139	Trihydroxy dodecadienoic acid	+	–	–	–	+	+
79	9.45	343.2129	$C_{18}H_{31}O_6^-$	−0.83	229, 211, 209, 171, 59	Tetrahydroxy octadecadienoic acid	–	+	+	+	+	+
80	9.47	187.0975	$C_9H_{15}O_4^-$	0.88	125, 123, 97	Nonanedioic acid (Azelaic acid)	+	+	+	+	+	+
82	9.78	299.1864	$C_{16}H_{27}O_5^-$	−0.55	201, 183, 143	Hydroxy hexadecenedioic acid	+	+	+	+	+	+
85	10.04	489.2703	$C_{24}H_{41}O_{10}^-$	0.35	327, 309, 291, 247, 229, 89, 71, 59	Trihydroxy octadecadienoic acid hexoside	+	+	+	+	+	+
86	10.05	375.2023	$C_{18}H_{31}O_8^-$	0.45	213, 195, 113, 101, 89, 71, 59	Oxo-dodecanoic acid hexoside	+	+	+	+	+	+
87	10.18	301.2021	$C_{16}H_{29}O_5^-$	−0.73	201, 183	Hydroxy hexadecanedioic acid	+	+	+	+	+	+
88	10.21	491.2856	$C_{24}H_{43}O_{10}^-$	1.13	329, 311, 293, 249, 229, 211, 101, 89, 59	Trihydroxy octadecenoic acid hexoside	+	+	+	+	+	+
90	10.34	201.1138	$C_{10}H_{17}O_4^-$	−1.61	161, 151, 139	Hydroxy decenoic acid	+	–	+	+	+	+
96	10.73	325.2015	$C_{18}H_{29}O_5^-$	1.73	233, 193, 141	Trihydroxy octadecatrienoic acid	+	–	+	–	+	–
97	10.85	327.2189	$C_{18}H_{31}O_5^-$	−3.08	309, 291, 229, 211, 183, 171	Trihydroxy octadecadienoic acid	+	+	+	+	+	+
98	10.98	677.4242	$C_{42}H_{61}O_5S^-$	0.54	327, 233	Trihydroxy octadecadienoic acid derivative	+	+	+	+	+	+
99	11.18	215.1287	$C_{11}H_{19}O_4^-$	−0.56	197, 153	Undecanedioic acid	+	+	–	+	+	–
101	11.38	329.2339	$C_{18}H_{33}O_5^-$	−1.29	229, 211, 183, 171	Trihydroxy octadecenoic acid	+	+	+	+	+	+
102	11.39	681.4557	$C_{42}H_{65}O_5S^-$	0.5	330, 329, 233	Trihydroxy octadecenoic acid derivative	+	+	+	+	+	+
103	11.61	227.1285	$C_{12}H_{19}O_4^-$	3.93	211, 183	Dodecanedioic acid	+	+	+	+	+	+
114	13.29	287.2233	$C_{16}H_{31}O_4^-$	−3.54	287, 269, 127	Dihydroxy hexadecanoic acid	+	–	–	–	+	–
116	13.33	309.2069	$C_{18}H_{30}O_4^-$	2.37	291, 221	Dihydroxy octadecatrienoic acid	+	+	+	+	+	+
119	13.42	311.2227	$C_{18}H_{31}O_4^-$	0.5	293, 275, 223, 201, 171	Dihydroxy octadecadienoic acid	+	+	+	+	+	+

(*continued on next page*)

Table 1 (*continued*)

#	t_r (min)	Molecular ion *m/z*	Molecular ion formula [M−H]$^-$	Error (ppm)	MS/MS fragments	Metabolite	lor	log	cr	ca	lr	lb
126	14.09	647.3280	$C_{30}H_{49}O_{12}^-$	1.33	277, 113, 101, 89, 71, 59	Dihexosyl octadecatrienoic acid *	+	–	+	+	+	+
127	14.10	313.2381	$C_{18}H_{33}O_4^-$	1.03	295, 277, 201, 183, 171, 127	Dihydroxy octadecenoic acid	+	+	–	+	+	+
129	14.44	639.4475	$C_{36}H_{63}O_9^-$	1.2	329, 327, 280, 229, 211, 171	Trihydroxy octadecadienoic acid derivative	+	–	+	–	+	–
133	14.69	699.3799	$C_{32}H_{59}O_{16}^-$	1.72	397, 255, 101, 89	Hexadecanoic acid derivative	+	+	+	+	+	+
134	14.75	325.2016	$C_{18}H_{29}O_5^-$	6.77	293, 275, 249	Trihydroxy octadecatrienoic acid	+	–	+	+	+	–
137	14.95	315.2545	$C_{18}H_{35}O_4^-$	−1.45	315, 297	Dihydroxy octadecanoic acid	+	–	–	–	–	–
138	14.96	807.5248	$C_{45}H_{75}O_{12}^-$	1.99	293, 277, 275, 235, 171, 121	Hydroxy octadecatrienoic acid derivative	+	+	+	–	–	–
140	15.02	293.2122	$C_{18}H_{29}O_3^-$	0.26	293, 275, 271, 97	Hydroxy octadecatrienoic acid	+	+	+	+	+	+
147	15.82	295.2277	$C_{18}H_{31}O_3^-$	0.1	295, 277, 259, 195, 171	Hydroxy octadecadienoic acid	+	+	+	+	+	+
148	16.00	277.2191	$C_{18}H_{29}O_2^-$	−7.16	277	Octadecatrienoic acid	+	+	–	–	–	–
149	16.07	505.3015	$C_{25}H_{45}O_{10}^-$	0.75	255, 113	Hexadecanoic acid derivative	+	+	–	+	+	–
161	17.59	271.1919	$C_{15}H_{27}O_4^-$	−1.5	199, 89	Pentadecanedioic acid	–	–	+	+	–	+
164	17.83	749.4839	$C_{35}H_{74}O_{14}P^-$	−8.01	489, 327, 309, 291, 277, 59	Trihydroxy octadecadienoic acid hexoside derivative	+	+	+	+	+	–
168	18.38	371.2442	$C_{20}H_{35}O_6^-$	−2.9	255, 101, 71	Diacetoxy hexadecanoic acid	+	–	–	–	+	–
170	18.42	277.2179	$C_{18}H_{29}O_2^-$	−1.8	277	Octadecatrienoic acid	+	+	+	–	–	–
171	18.45	271.2285	$C_{16}H_{31}O_3^-$	−2.19	271, 253, 225	Hydroxy hexadecanoic acid	+	+	+	+	+	+
173	18.61	591.4617	$C_{36}H_{63}O_6^-$	2.82	279, 211	Octadecadienoic acid derivative	–	+	–	–	–	+
181	19.34	279.2332	$C_{18}H_{31}O_2^-$	−0.83	279, 97	Octadecadienoic acid	+	+	+	+	+	+
186	20.49	587.4318	$C_{36}H_{59}O_6^-$	0.1	277, 211	Octadecatrienoic acid derivative	+	+	+	+	+	+
187	21.27	383.3533	$C_{24}H_{47}O_3^-$	−0.57	337	Hydroxy tetracosanoic acid	–	+	+	+	+	+
Lipids												
2	0.90	333.0591	$C_9H_{18}O_{11}P^-$	0.21	333, 259, 241, 171, 153, 79	Phosphatidyl-myoinositol	+	–	+	+	+	+
100	11.26	609.2583	$C_{27}H_{45}O_{13}S^-$	−2.1	563, 523, 483, 371, 225, 81, 80	Sulfoquinovosyl monoacyl glycerol (18:3[OH])	–	–	–	+	+	+
104	11.87	479.2046	$C_{21}H_{36}O_{10}P^-$	0.89	293, 171, 153, 79	Monoacyl phosphoglyceride (18:3[3OH])	+	+	+	+	+	+
105	12.39	999.4648	$C_{45}H_{75}O_{24}^-$	0.77	559, 383, 277, 179, 89	Tetrahexosyl monoacyl glycerol (18:3)	+	+	+	+	+	+
106	12.46	593.2729	$C_{27}H_{46}O_{12}P^-$	0.8	277, 241, 153, 79	Monoacyl phosphatidyl-myoinositol (18:3)	+	+	+	+	+	+
107	12.50	527.2533	$C_{23}H_{43}O_{11}S^-$	1.22	527, 299, 227, 225, 165, 81	Sulfoquinovosyl monoacyl glycerol (14:0)	+	+	+	+	+	–
108	12.58	577.2700	$C_{27}H_{45}O_{11}S^-$	−2.14	577, 299, 277, 225, 165, 81	Sulfoquinovosyl monoacyl glycerol (18:3)	+	+	+	+	+	+
109	12.84	837.4116	$C_{39}H_{65}O_{19}^-$	1.32	577, 397, 277, 221, 179, 161, 113, 101, 89, 71, 59	Trihexosyl monoacyl glycerol (18:3)	+	+	+	+	+	+
110	12.85	553.2686	$C_{25}H_{45}O_{11}S^-$	0.38	555, 299, 255, 225, 165, 81	Sulfoquinovosyl monoacyl glycerol (16:1)	+	+	+	+	+	+
111	12.99	595.2889	$C_{27}H_{48}O_{12}P^-$	0.18	279, 241, 153, 79	Monoacyl phosphatidyl-myoinositol (18:2)	+	+	+	+	+	+
112	13.02	541.2688	$C_{24}H_{45}O_{11}S^-$	0.43	541, 299, 241, 225, 165, 81	Sulfoquinovosyl monoacyl glycerol (15:0)	+	+	+	+	+	–
113	13.11	579.2844	$C_{27}H_{45}O_{11}S^-$	0.23	579, 299, 279, 225, 165, 81	Sulfoquinovosyl monoacyl glycerol (18:2)	+	+	+	+	+	+
115	13.30	675.3606	$C_{33}H_{55}O_{14}^-$	−0.45	397, 277, 253, 113, 101, 89, 59	Dihexosyl monoacyl glycerol (18:3)	+	+	+	+	+	+
117	13.38	571.2887	$C_{25}H_{48}O_{12}P^-$	0.21	315, 255, 241, 153, 79	Monoacyl phosphatidyl-myoinositol (16:0)	+	+	+	+	+	+
118	13.41	987.5885	$C_{51}H_{87}O_{18}^-$	1.14	397, 311, 293, 277, 275, 223, 201, 171	Dihexosyl monoacyl glycerol (18:2[2OH]/18:3[OH])	+	–	–	–	–	–
120	13.43	555.2855	$C_{25}H_{47}O_{11}S^-$	−1.86	555, 299, 255, 225, 165, 81	Sulfoquinovosyl monoacyl glycerol (16:0)	+	+	+	+	+	+
122	13.83	581.2992	$C_{27}H_{49}O_{11}S^-$	1.9	581, 299, 281, 225, 165, 81	Sulfoquinovosyl monoacyl glycerol (18:1)	+	+	+	+	+	+
123	13.85	597.3028	$C_{27}H_{50}O_{12}P^-$	2.16	281, 241, 153	Monoacyl phosphatidyl-myoinositol (18:1)	+	–	+	+	–	–
124	13.90	505.2568	$C_{24}H_{42}O_9P^-$	1.95	277, 153, 79	Monoacyl phosphatidyl-glycerol (18:3)	+	+	+	+	+	+
125	13.99	723.3787	$C_{33}H_{57}O_{14}^-$	2.67	397, 279, 235, 113, 101, 89, 59	Dihexosyl monoacyl glycerol (18:2) *	+	+	+	+	+	+
128	14.19	638.3306	$C_{29}H_{53}NO_{12}P^-$	−8.93	476, 279, 153, 79	Hexosyl monoacyl phosphatidyl-ethanolamine (18:2)	+	+	–	+	+	–
130	14.61	583.3159	$C_{27}H_{51}O_{11}S^-$	0.18	583, 299, 283, 225, 165, 81	Sulfoquinovosyl monoacyl glycerol (18:0)	+	+	+	+	+	+
131	14.65	653.3758	$C_{31}H_{57}O_{14}^-$	1.16	255	Dihexosyl monoacyl glycerol (16:0)	+	–	+	+	+	–
132	14.66	614.3305	$C_{27}H_{53}NO_{12}P^-$	0.87	452, 255, 153, 79	Hexosyl monoacyl phosphatidyl-ethanolamine (16:0)	+	+	–	+	+	–
135	14.82	507.2724	$C_{24}H_{44}O_9P^-$	1.19	279, 153, 79	Monoacyl phosphatidyl-glycerol (18:2)	+	+	+	+	+	+

(*continued on next page*)

Table 1 (*continued*)

#	t_r (min)	Molecular ion *m/z*	Molecular ion formula [M−H]$^-$	Error (ppm)	MS/MS fragments	Metabolite	lor	log	cr	ca	lr	lb
136	14.83	513.3056	$C_{27}H_{45}O_9^-$	7.22	277, 255, 253, 161, 89, 59	Hexosyl monoacyl glycerol (18:3)	+	+	+	+	–	+
139	14.99	481.2574	$C_{22}H_{42}O_9P^-$	−0.00	253, 245, 227, 171, 153, 79	Monoacyl phosphatidyl-glycerol (16:1)	+	+	+	+	+	+
141	15.04	431.2207	$C_{21}H_{36}O_8P^-$	−0.63	277, 153, 79	Monoacyl phosphoglyceride (18:3)	+	+	+	+	+	+
142	15.28	381.2308	$C_{17}H_{34}O_7P^-$	0.23	381, 153, 97, 79	Mononacyl phosphoglyceride (14:0)	+	–	–	+	–	+
143	15.44	476.2771	$C_{23}H_{43}NO_7P^-$	−1.36	279, 196, 171, 153	Monoacyl phosphatidyl-ethanolamine (18:2)	+	+	+	+	+	–
144	15.54	529.3022	$C_{27}H_{45}O_{10}^-$	1.45	279, 249	Glycerolipid derivative (18:2)	+	+	–	+	+	+
145	15.57	561.3281	$C_{27}H_{47}O_9^-$	0.47	279, 253	Hexosyl monoacyl glycerol (18:2) *	+	+	+	+	+	+
146	15.77	483.2726	$C_{22}H_{44}O_9P^-$	−5.12	255, 153, 79	Monoacyl phosphatidyl-glycerol (16:0)	+	+	+	+	+	+
150	16.26	853.4766	$C_{45}H_{73}O_{13}S^-$	−0.55	853, 575, 277, 225, 165, 81	Sulfohexosyl diacyl glycerol (18:3/18:3)	+	–	+	+	+	–
151	16.26	869.4716	$C_{45}H_{73}O_{14}S^-$	6.97	823, 743, 559, 277, 225, 81, 80	Sulfoquinovosyl diacyl glycerol (18:3/18:3[OH])	–	–	–	–	+	+
152	16.39	433.2365	$C_{21}H_{38}O_7P^-$	−0.77	279, 171, 153, 79	Monoacyl phosphoglyceride (18:2)	+	+	+	+	+	+
153	16.40	815.4980	$C_{43}H_{75}O_{12}S^-$	1.74	815, 559, 537, 277, 255, 225, 165, 95, 81	Sulfoquinovosyl diacyl glycerol (16:0/18:3)	–	+	+	+	+	–
154	16.65	407.2204	$C_{19}H_{36}O_7P^-$	0.6	171, 153, 79	Monoacyl phosphoglyceride (16:1)	+	+	+	+	+	+
155	16.67	452.2781	$C_{21}H_{43}NO_7P^-$	0.98	255, 196, 79	Monoacyl phosphatidyl-ethanolamine (16:0)	+	–	–	+	+	–
156	16.76	445.2360	$C_{22}H_{38}O_7P^-$	−0.57	277, 167, 79	Monoacyl phosphoglyceride (18:3) methyl ester	+	–	+	+	+	–
157	16.95	1097.6248	$C_{57}H_{93}O_{20}^-$	3.35	919, 559, 415, 397, 277, 226	Trihexosyl diacyl glycerol (18:3/18:3)	–	–	–	–	+	–
158	17.50	833.5171	$C_{43}H_{78}O_{13}P^-$	2.23	279, 255, 242, 153, 79	Diacyl phosphatidyl-myoinositol (16:0/18:2)	–	+	+	+	+	–
159	17.53	843.5289	$C_{45}H_{79}O_{12}S^-$	1.61	843, 559, 225, 165, 81	Sulfoquinovosyl diacyl glycerol (18:3/18:0)	–	+	–	–	–	–
160	17.57	847.4872	$C_{43}H_{75}O_{14}S^-$	1.87	801, 761, 721, 537, 279, 255, 225, 165, 95, 81	Sulfoquinovosyl diacyl glycerol (16:0/18:3[2OH])	–	–	–	–	+	+
162	17.59	831.4979	$C_{43}H_{76}O_{13}P^-$	3.79	277, 255, 241, 81, 79	Diacyl phosphatidyl-myoinositol (16:0/18:3)	+	–	+	+	+	+
163	17.73	409.2361	$C_{19}H_{38}O_7P^-$	0.08	255, 153, 79	Monoacyl phosphoglyceride (16:0)	+	–	+	+	+	+
165	18.07	867.4701	$C_{43}H_{75}O_{13}S^-$	2.5	831, 575, 537, 225, 165, 81	Sulfohexosyl diacyl glycerol (16:0/18:3) **	+	–	–	–	–	–
166	18.11	760.5588	$C_{41}H_{78}NO_{11}^-$	0.52	552, 534, 281, 101, 89, 59	Hexosyl ceramide (17:0[3OH]/18:1)	–	–	+	+	–	+
167	18.33	435.2516	$C_{21}H_{40}O_7P^-$	0.02	281, 153, 79	Monoacyl phosphoglyceride (18:1)	+	+	+	+	+	+
169	18.41	693.4496	$C_{39}H_{66}O_8P^-$	−0.35	279, 277, 153, 79	Diacyl phosphoglyceride (18:2/18:3)	–	–	–	+	+	+
172	18.53	837.4845	$C_{45}H_{73}O_{12}S^-$	−1.81	837, 559, 277, 225, 165, 81	Sulfoquinovosyl diacyl glycerol (18:3/18:3)	+	+	+	+	+	+
174	18.87	951.5660	$C_{51}H_{83}O_{16}^-$	3.06	293, 277, 235, 101, 59	Dihexosyl diacyl glycerol (18:3/18:3[OH])	–	–	+	+	–	–
175	19.01	787.4680	$C_{41}H_{71}O_{12}S^-$	0.45	787, 559, 277, 225, 165, 95, 81	Sulfoquinovosyl diacyl glycerol (14:0/18:3)	–	–	+	–	–	–
176	19.02	741.4348	$C_{39}H_{66}O_{11}P^-$	1.64	325, 293, 279, 277, 249, 153, 79	Diacyl phosphoglyceride (18:2/18:3[3OH])	–	–	–	–	–	+
177	19.02	819.5255	$C_{46}H_{75}O_{12}^-$	1.12	277	Hexosyl diacyl glycerol (18:3/18:3) *	–	+	+	+	–	–
178	19.24	447.2516	$C_{22}H_{40}O_7P^-$	0.12	279, 167, 79	Monoacyl phosphoglyceride (18:2) methyl ester	+	–	+	+	+	+
179	19.27	817.5132	$C_{43}H_{77}O_{12}S^-$	0.78	817, 561, 537, 279, 255, 225, 165, 95, 81	Sulfoquinovosyl diacyl glycerol (16:0/18:2)	–	+	+	+	+	+
180	19.28	813.4818	$C_{43}H_{73}O_{12}S^-$	1.17	813, 535, 277, 225, 165, 95, 81	Sulfoquinovosyl diacyl glycerol (16:1/18:3)	+	+	–	+	+	–
182	19.35	691.4340	$C_{39}H_{64}O_8P^-$	0.55	277, 153, 79	Diacyl phosphoglyceride (18:3/18:3)	+	+	+	–	–	+
183	19.44	669.4489	$C_{37}H_{66}O_8P^-$	2.09	277, 255, 153, 79	Diacyl phosphoglyceride (16:0/18:2)	–	–	–	–	–	+
184	19.52	839.4981	$C_{45}H_{75}O_{12}S^-$	0.45	839, 561, 279, 277, 225, 165, 81	Sulfoquinovosyl diacyl glycerol (18:2/18:3)	+	+	+	+	+	+
185	19.77	981.5765	$C_{51}H_{83}O_{15}^-$	1.95	397, 277	Dihexosyl diacyl glycerol (18:3/18:3) *	–	+	–	–	+	+
188	21.66	695.4661	$C_{39}H_{68}O_8P^-$	2.84	279, 153, 79	Diacyl phosphoglyceride (18:2/18:2)	–	–	–	–	+	+

(*continued on next page*)

Table 1 (*continued*)

#	t_r (min)	Molecular ion *m/z*	Molecular ion formula [M−H]$^-$	Error (ppm)	MS/MS fragments	Metabolite	lor	log	cr	ca	lr	lb
189	21.71	815.4991	$C_{43}H_{75}O_{12}S^-$	−0.74	815, 559, 277, 255, 225, 165, 81	Sulfoquinovosyl diacyl glycerol (16:0/18:3)	+	+	+	+	+	+
190	21.79	793.5161	$C_{41}H_{77}O_{12}S^-$	−0.56	793, 537, 255, 225, 165, 95, 81	Sulfoquinovosyl diacyl glycerol (16:0/16:0)	–	+	–	–	–	+
191	21.91	841.5142	$C_{45}H_{77}O_{12}S^-$	3.42	841, 561, 559, 279, 225, 165, 81	Sulfoquinovosyl diacyl glycerol (18:2/18:2)	+	–	+	+	–	–
192	21.93	833.5167	$C_{43}H_{78}O_{13}P^-$	1.55	279, 255, 241, 153, 79	Diacyl phosphatidyl-myoinositol (16:0/18:2)	–	–	–	+	–	–
193	22.01	843.5290	$C_{45}H_{79}O_{12}S^-$	−0.16	843, 559, 225, 165, 81	Sulfoquinovosyl diacyl glycerol (18:3/18:0)	–	+	–	–	–	–
194	22.05	959.5932	$C_{49}H_{85}O_{15}^-$	2.07	397, 277, 255	Dihexosyl diacyl glycerol (16:0/18:3) *	–	–	–	+	+	–
195	22.57	562.3150	$C_{27}H_{49}NO_9P^-$	1.33	277, 79	Monoacyl phosphatidyl-choline derivative (18:3)	+	–	–	+	+	–

Lor, var. *longifolia* red; **log**, var. *longifolia* green; **cr**, var. *crispa*; **ca**, var. *capitata*; **lr**, var. *lolla rosa*; and **lb**, var. *lolla bionda*; * Formic acid adduct; ** chloride adduct; *** other adduct; +, present; -, absent.

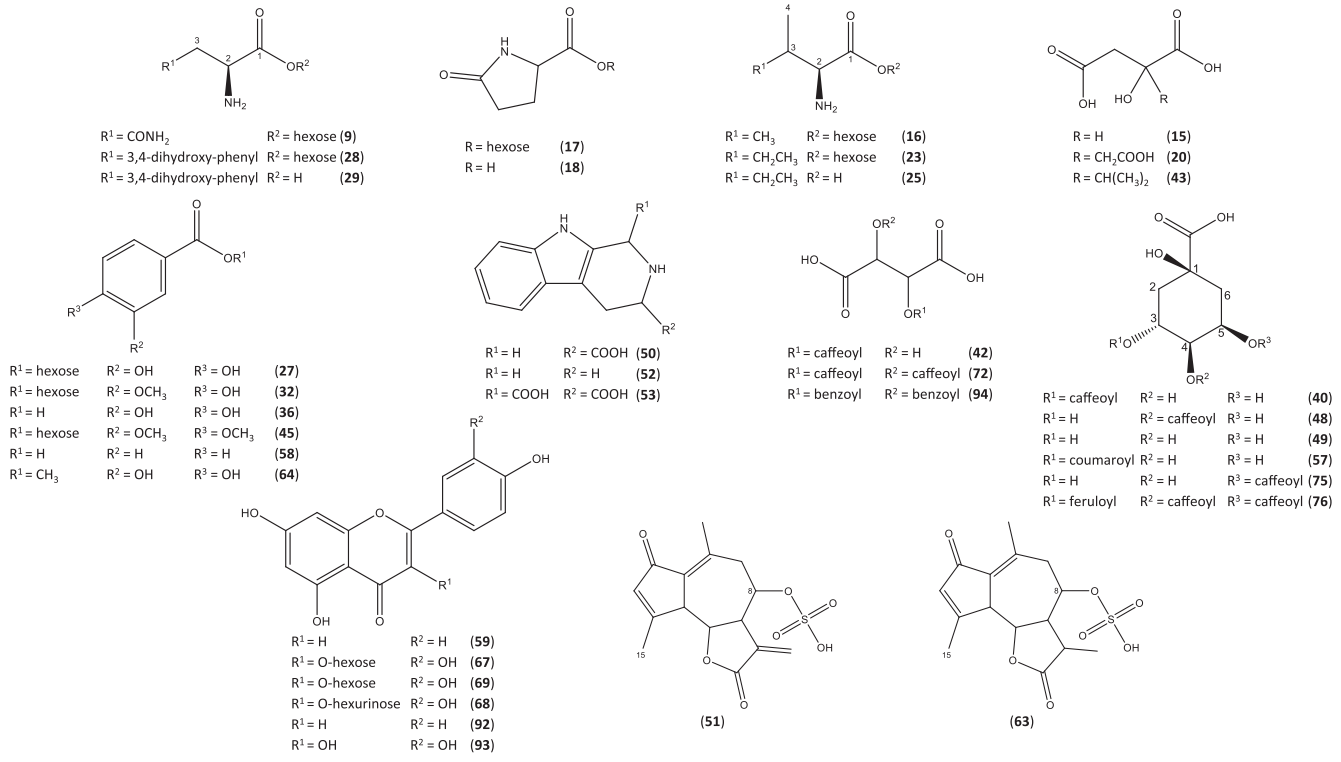

Fig. 1. Structures of the main primary and secondary metabolites tentatively identified in the methanol extracts of *L. sativa* by LC-MS/MS. Carbon numbering system for each metabolite is based on analogy rather than IUPAC rules. Metabolite numbers follow those listed in Table 1.

353.0873 ($C_{16}H_{17}O_9$)$^-$], respectively) could be easily distinguished by their base peaks at *m/z* 191 formed after the loss of a caffeoyl moiety (Suppl. Fig. S5). Additionally, it was possible to discriminate between the two isomers (5- and 3-caffeoyl quinic acids) by a distinctly intense ion at *m/z* 179 corresponding to the deprotonated caffeic acid in 3-caffeoyl quinic acid. Other chlorogenic acids detected were 3-coumaroyl quinic acid, peak **57** [*m/z* 337.0931 ($C_{16}H_{17}O_8$)$^-$], showing a base peak at *m/z* 191 (characteristic of 3-acyl quinic acids) and 3,4-dicaffeoyl quinic acid, peak **76** [*m/z* 515.1194 ($C_{25}H_{23}O_{12}^-$)], with a base peak at *m/z* 173 and secondary intense ions at *m/z* 179 and 191 justifying vicinal caffeoyl moieties on C-3 and C-4 (Suppl. Fig. S6-S7).

LC-MS/MS analysis also revealed the presence of several hydroxylated and methoxylated benzoic acids (Table 1), where characteristic losses of CO_2 (*m/z* 44), CO (*m/z* 28), CH_3 (*m/z* 14), and OCH_3 (*m/z* 30) were observed. In detail, peak **36** [*m/z* 153.019 ($C_7H_5O_4$)$^-$] showed a base peak at *m/z* 109 resulting from the loss of CO_2 group [M−44]$^-$ and was annotated as dihydroxy benzoic acid (Suppl. Fig. S8). Similarly, the spectra of peaks **27** [*m/z* 315.0734 ($C_{13}H_{15}O_9$)$^-$] and **64** [*m/z* 167.0349 ($C_8H_7O_4$)$^-$] revealed an intense ion at *m/z* 152 indicating dihydroxy benzoic acid moiety. This fragment is formed after the loss of a hexose sugar in metabolite **27** [M−162−H]$^-$ and a methyl group [M−14−H]$^-$ in **64**, leading to their annotation as dihydroxy benzoic acid hexoside and dihydroxy methyl benzoate, respectively (Suppl. Fig. S9-S10).

Other phenolic acids detected were caffeoyl tartaric acid, peak **42** [*m/z* 311.0404 ($C_{13}H_{11}O_9$)$^-$] and dicaffeoyl tartaric acid, peak **72** [*m/z* 473.0724 ($C_{22}H_{17}O_{12}$)$^-$], both revealing a characteristic ion peak at *m/z* 149 due to the loss of 1 caffeoyl [M−162]$^-$ and 2 caffeoyl [M−2*162]$^-$ moieties, respectively (Suppl. Fig. S11-S12). Molecular networking showed the presence of some caffeoyl derivatives (cluster G), such as 4-caffeoyl quinic (**48**), caffeoyl tartaric (**72**), and 3,4-dicaffeoyl quinic (**76**) acids (Suppl. Fig. S25).

3.1.5. Flavonoids

Flavonoids are the most abundant group of plant metabolites, they play a vital role in plant physiology and are commonly found as *O*-glycosides bound to one or more sugar moieties (Ferreyra et al., 2012). For the *O*-glucosyl flavonoids the most intense fragment results from the loss of the sugar unit, *i.e.,* hexose (*m/z* 162), (*m/z* 146), pentose (*m/z* 132), deoxyhexose (*m/z* 146), or hexuronic acid (*m/z* 176) (Simirgiotis et al., 2012).

The MS/MS spectra of peak **67** [*m/z* 447.0933 ($C_{21}H_{19}O_{11}$)$^-$] and **68** [*m/z* 463.0883 ($C_{21}H_{19}O_{12}^-$)] showed loss of the attached hexose unit and revealed base peaks at *m/z* 300 (quercetin) and 284 (kaempferol), respectively, confirming the *O*-hexosyl flavonoid (Table 1 & Suppl. Fig. S13). A higher abundant ion [M−162−H]$^-$ (at *m/z* 284 in peak **67** and 300 in **68**), derived from a homolytic cleavage, relative to the corresponding ion [M−162]$^-$ (at *m/z* 285 in compound **67** and 301 in **68**), derived from a heterolytic cleavage, suggests 3-*O*-glycosylation and led to the characterization of peaks **67** and **68** as kaempferol 3-*O*-hexoside and quercetin 3-*O*-hexoside, respectively (Otify et al., 2023). Other flavonoids annotated were apigenin (**59**) [*m/z* 269.0476 ($C_{15}H_9O_5^-$)], kaempferol hexuronide (**69**) [*m/z* 461.0727 ($C_{21}H_{17}O_{12}^-$)], luteolin (**92**) [*m/z* 285.0402 ($C_{15}H_9O_6^-$)], and quercetin (**93**) [*m/z* 301.0353 ($C_{15}H_9O_7^-$)] (Table 1 & Suppl. Fig. S14). A few flavonoids appeared as self-looped nodes in the established molecular network (Suppl. Fig. S25).

3.1.6. Fatty acids

LC-MS/MS analysis also revealed many hydroxylated fatty acids (oxylipids), *e.g.*, peaks **85**, **88**, **97**, **119**, and **147** (Table 1), which mainly constituted clusters C & F in the molecular network (Suppl. Fig. S25). Primary fragmentation of most fatty acids showed neutral loss(s) of water followed by decarboxylation (Yang et al., 2013). In detail, Peaks **85** [*m/z* 489.2703 ($C_{24}H_{41}O_{10}$)$^-$] and **88** [*m/z* 491.2856 ($C_{24}H_{43}O_{10}$)$^-$] displayed similar fragmentation patterns with distinctive ions at *m/z* 327 and 329, respectively, after the loss of the attached sugar unit [M−162]$^-$ (Suppl. Fig. S15-S16). Moreover, peak **85** exhibited a mass difference of 2 *m/z* with respect to **88** suggesting an extra double bond, hence both were assigned as trihydroxy octadecadienoic acid hexoside and trihydroxy octadecenoic acid hexoside, respectively. Peaks **97** [*m/z* 327.2189 ($C_{18}H_{31}O_5$)$^-$], **119** [*m/z* 311.2227 ($C_{18}H_{31}O_4$)$^-$], and **147** [*m/z* 295.2277 ($C_{18}H_{31}O_3$)$^-$], with a mass difference of 16 *m/z* indicative of an extra hydroxyl group, were annotated as trihydroxy, dihydroxy, and hydroxy octadecadienoic acids, respectively (Suppl. Fig. S17-S19). Fatty acids are the first substantial structural components of lipids, and they constitute the main skeleton of plant cell membranes. There is a growing interest in oxylipids in foodstuff due to their cytotoxic, anti-inflammatory, and anti-microbial activities (Martin-Arjol et al., 2010).

3.1.7. Lipids and their derivatives

Biological systems, such as plant cells, involve thousands of individual molecular lipid species, named the lipidome of an organism. Lipids have a variety of functions including structural components for the integrity of cell membranes, energy storage, and signaling mediators in plant defense systems (Fahy et al., 2009). Besides, they are important constituents that significantly affect food quality even if present at minor concentrations, which can vary among plant species and derived foods (German et al., 1999).

Neutral lipids are poorly soluble in water, but polar lipids solubilize to a certain extent in polar solvents, such as methanol (Ibrahim et al., 2023; Otify et al., 2023; Saini et al., 2021). They can be categorized into several classes such as glycerolipids, phospholipids, sulfolipids, and sphingolipids. Structurally, the acyl group of the fatty acid is esterified with glycerol (glycerolipids), or phosphoglycerol (phospholipids) to produce several derivatives. Sometimes, choline, myoinositol, or ethanolamine, may be linked to the phosphate group resulting in a great variation of phospholipid structures. Sulfolipids are a class of lipids in which a sulfated sugar (mostly quinovose or glucose) is bonded to acylglycerol (Calvano et al., 2020).

Recently, LC-MS/MS has been widely applied to characterization of food lipids due to its high selectivity and sensitivity (Köfeler et al., 2012). In the negative ESI mode, the presence of carboxylate ions [RCOO]$^-$ recognizes the individual fatty acids esterified on the glycerol skeleton, *e.g.*, *m/z* 255 for hexadecanoic acid (16:0), 277 for octadecatrienoic acid (18:3), and 293 for hydroxy octadecatrienoic acid (18:3 [OH]). Moreover, the appearance of some diagnostic ions corresponding to specific functional moieties helps to the characterization of the lipid type, *i.e.*, *m/z* 79 (phosphonate), 81 (sulfonate), 153 (phospho-glycerol), 196 (phosphatidyl-ethanolamine), 225 (sulfoquinovosyl–18), 241 (phospho-myoinositol), and 397 (dihexosyl glycerol).

A total of 70 lipids were tentatively identified in the investigated samples becoming the most numerous class of annotated metabolites, and as far as we know, the first comprehensive report on the fragmentation pattern of lipids and fatty acids in the examined 6 lettuce varieties. For instance, peaks **106** [*m/z* 593.2729 ($C_{27}H_{46}O_{12}P$)$^-$], **115** [*m/z* 675.3606 ($C_{33}H_{55}O_{14}$)$^-$], **141** [*m/z* 431.2207 ($C_{21}H_{36}O_8P$)$^-$], **155** [*m/z* 452.2781 ($C_{21}H_{43}NO_7P$)$^-$], and **189** [*m/z* 815.4991 ($C_{43}H_{75}O_{12}S$)$^-$] were annotated as monoacyl phosphatidyl-myoinositol (18:3), dihexosyl monoacyl glycerol (18:3), monoacyl phosphoglyceride (18:3), monoacyl phosphatidyl-ethanolamine (16:0), and sulfoquinovosyl diacyl glycerol (16:0/18:3), respectively (Suppl. Fig. S20-S24). In detail, the MS/MS spectrum of peak **115** showed a base peak at *m/z* 277 (18:3 fatty acid) and a fragment ion at *m/z* 397 (dihexosyl glycerol) and was annotated as dihexosyl monoacyl glycerol (18:3) (Suppl. Fig. S20). Peaks **106** and **141** showed similar fragments at *m/z* 79, 153, and 277 indicating a monoacyl phosphoglyceride (18:3). Additionally, the spectrum of peak **106** revealed an extra intense ion at *m/z* 241 diagnostic of a phospho-myoinositol moiety (Suppl. Fig. S21-S22). Accordingly, peaks **106** and **141** were annotated as monoacyl phosphatidyl-myoinositol (18:3) and monoacyl phosphoglyceride (18:3), respectively. Peak **155** revealed ions characteristic of hexadecenoic acid (*m/z* 255) and phospho-glycerol (*m/z* 79), in addition to phosphatidyl-ethanolamine (*m/z* 196) and was assigned as monoacyl phosphatidyl-ethanolamine (16:0) (Suppl. Fig. S23), while peak **189** was annotated as sulfoquinovosyl diacyl glycerol (16:0/18:3), where its MS/MS spectrum showed the diagnostic ions for 16:0 (*m/z* 255) and 18:3 fatty acids (*m/z* 277) and a sulfoquinovosyl moiety (*m/z* 81 and 225) (Suppl. Fig. S24). A significant number of lipids were grouped in clusters A & B of the molecular network (Suppl. Fig. S25).

3.2. Determination of the antibacterial activity

Lettuce leaves are rich in antibacterial constituents and breeding methods are primarily focused on various morphological features and resistance against diseases (Pink & Keane, 1993). However, a better understanding of the correlation between lettuce antibacterial effect and its composition is necessary to promote lettuce varieties enriched in natural antibacterials and further improve future breeding programs.

All lettuce varieties showed significant antibacterial activity against both MSSA and MRSA strains ($p < 0.0001$, ANOVA) relative to the negative control with pure DMSO (Suppl. Table S3 & Suppl. Fig. S26). The antibacterial activity was slightly lower compared to CIP and there was no significant difference among the six tested extracts.

3.3. Determination of the antihemolytic effect

Most lettuce varieties exhibited significant antihemolytic effect towards both *S. aureus strains* (Fig. 2). For MSSA, **lr**, **lb**, and **cr** varieties exhibited the greatest antihemolytic effect against the staphylococcal hemolysins causing a significant reduction in hemolysis (>99%). The antihemolytic effect of **log**, **lor**, and **ca** was a little bit lower than the others (96%, 91%, and 89%, of hemolysis reduction, respectively). In the case of MRSA, the hemolysis was reduced by ~ 90% by **lor** and **ca**, and by 80%, 75%, and 70% by **lb**, **lr**, and **log** varieties, respectively.

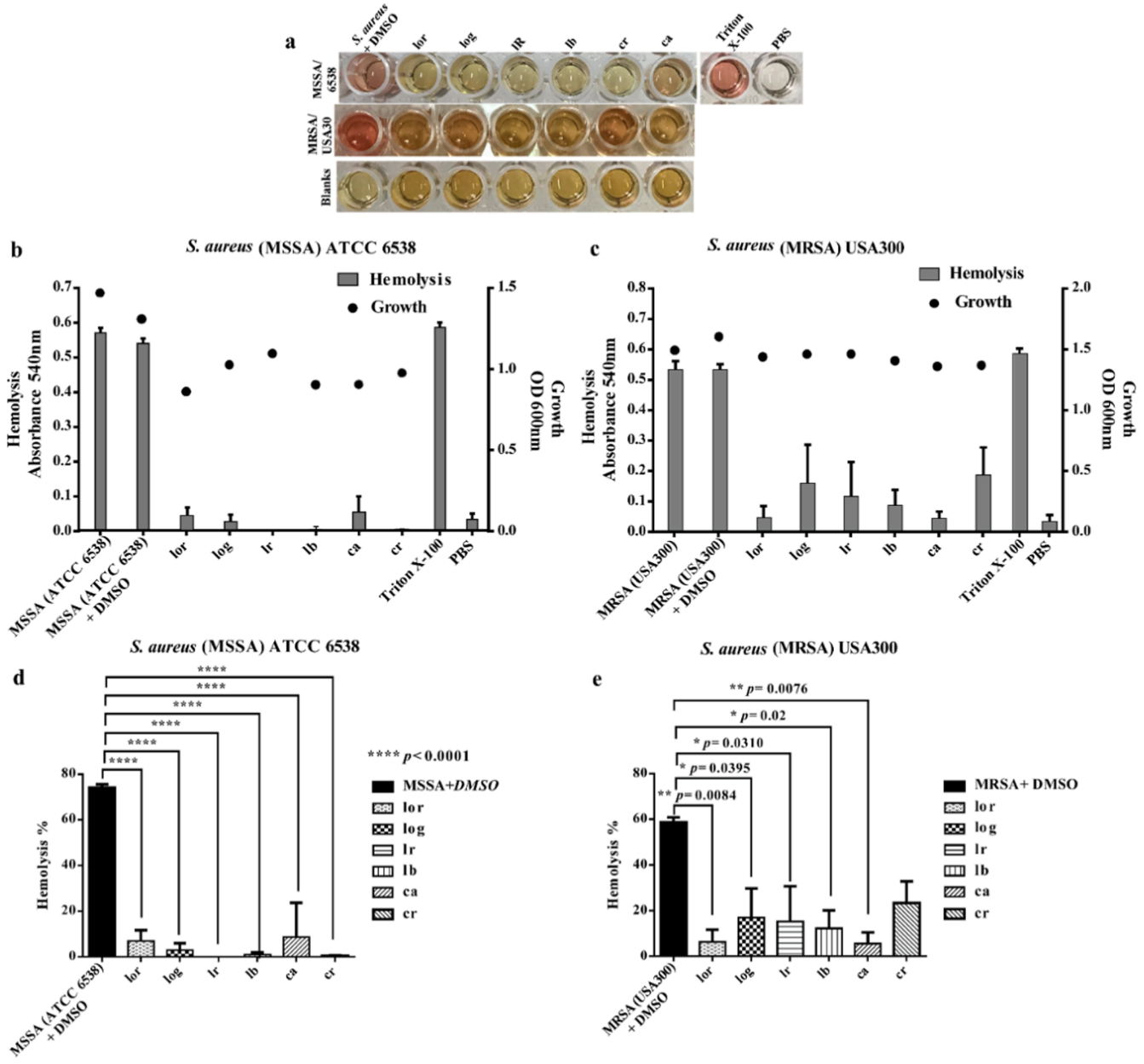

Fig. 2. Antihemolytic effect of *L. sativa* varieties against hemolysin production of the studied *S. aureus* strains. (**a**) Representative photograph of the culture supernatants after overnight incubation with and without the different *L. sativa* extracts and controls. (**b** & **c**) Effect on the growth and hemolysin production in MSSA ATCC 6538 (**b**) and MRSA USA300 (**c**) strains. (**d** & **e**) Percentage of hemolysis in MSSA ATCC 6538 (**d**) and MRSA USA300 (**e**) strains. The percentage of hemolysis was calculated relative to Triton X-100 (reference control for hemolysis) after normalizing the measured absorbance at 540 nm by the optical density (OD) of growth at 600 nm. The hemolytic effect of *S. aureus* cultures, exposed to only DMSO and PBS was considered as reference and negative controls, respectively. All experiments were performed in triplicate. Asterisks (*) indicate statistically significant differences (at $p < 0.05$), in comparison to *S. aureus* strains with DMSO as determined by ANOVA followed by *post-hoc t*-test.

Finally, **cr** lettuce exhibited the lowest antihemolytic effect (60% of hemolysis reduction) against MRSA, which was non-significant compared to the untreated strain.

3.4. Determination of transcriptional levels of hla gene

The six lettuce varieties exhibited different levels of antibacterial and antihemolytic activities against MSSA and MRSA strains except for the **cr** variety, which showed a non-significant antihemolytic effect against MRSA (Fig. 2). However, no significant differences were expected phenotypically among the six varieties regarding their antibacterial and antihemolytic activities. In order to obtain complementary information, four varieties with high (**ca**), middle (**lor** and **log**), and low (**cr**) antihemolytic effect, were selected to investigate the *hla* transcriptional levels. qPCR revealed that all the tested varieties exhibited significant downregulation of *hla* transcriptional level ($p < 0.05$, ANOVA) in both MSSA and MRSA relative to the control with pure DMSO, except for **cr** in MRSA that, in accordance with our previous finding about the antihemolytic effect (Fig. 2), showed a non-significant reduction (Fig. 3). In contrast, **ca**, **lor**, and **log** lettuces exhibited a great reduction in *hla* transcript-level in MRSA, by 13.0, 9.7, and 6.7 folds, respectively (Fig. 3b). However, it is worth highlighting that the differences on *hla* reduction levels between MSSA and MRSA upon exposure to lettuce varieties may be related to the differences on the original *hla* transcription levels of the studied strains (result not shown).

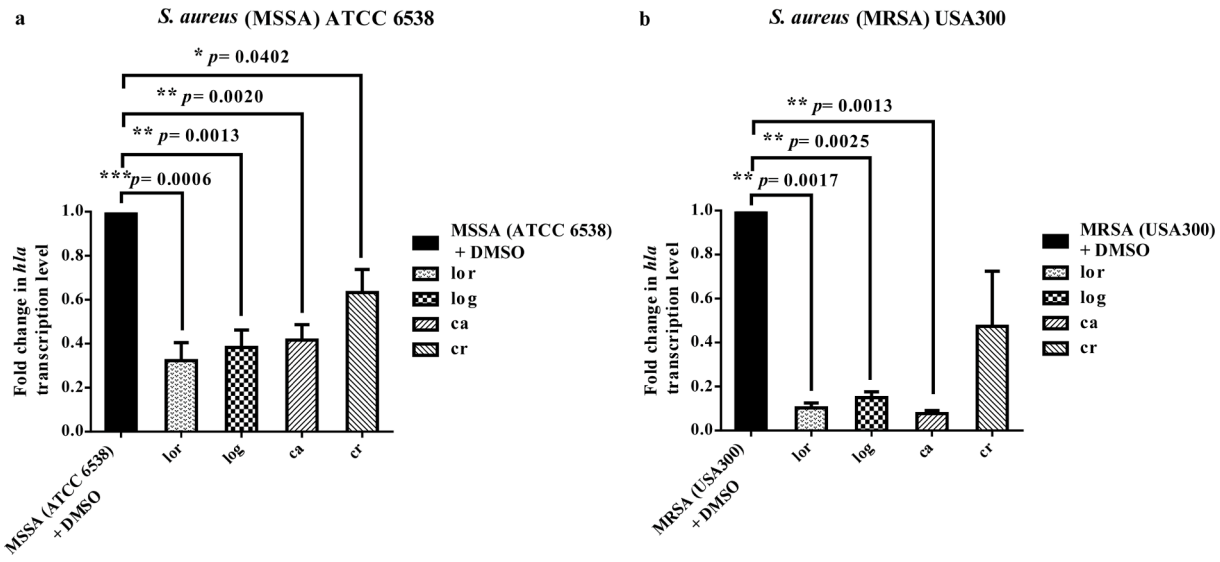

Fig. 3. Quantitative analysis of *hla* transcriptional level of *S. aureus* upon exposure to sub-inhibitory concentrations of the extracts of the different *L. Sativa* varieties. (**a**) MSSA ATCC 6538 and (**b**) MSRA USA300 strains. The bar chart represents the fold change in the transcriptional level of *hla* gene upon exposure to **lor**, **log**, **ca**, and **cr** extracts. Either MSSA or MRSA culture exposed to DMSO only (the solvent) was considered as a calibrator. Fold change was calculated using the ΔΔCt method. Asterisks (*) indicate statistically significant differences (at $p < 0.05$), in comparison to *S. aureus* as determined by ANOVA followed by *post-hoc t*-test.

3.5. Multivariate data analyses

Upon visual examination of the LC-MS chromatograms (Suppl. Fig. S1), the 6 lettuce varieties exhibited some notable differences. Then, multivariate data analysis (*i.e.*, unsupervised PCA and supervised OPLS-DA) was applied to classify the samples into distinct groups while revealing their characteristic metabolite distribution (Saber et al., 2021).

3.5.1. Principal component analysis (PCA)

With no pre-knowledge of the dataset, PCA is a data reduction method that is mainly applied in omics sciences for sample classification into different groups in compliance with their chemical profiles. To assess the relative chemical profiles variance among the studied lettuce

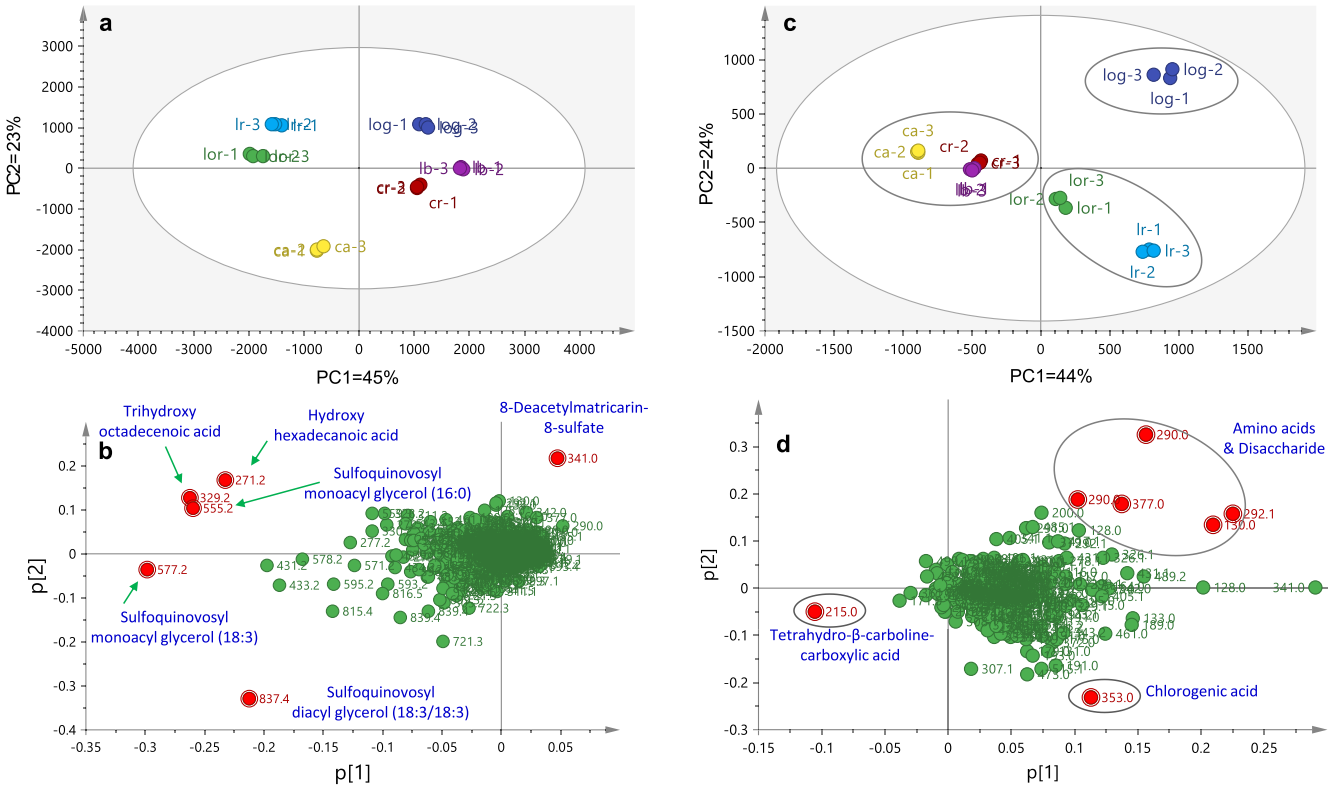

Fig. 4. LC-MS based PCA of the six *L. sativa* varieties ($n = 3$). (**a**) Score and (**b**) loading plots for PC1 and PC2 (t_r 0–24 min). (**c**) Score and (**d**) loading plots for PC1 and PC2 (t_r 0–10.76 min). The metabolites showing the largest absolute score values along each PC are named and colored in red. (For interpretation of the references to color in this figure legend, the reader is referred to the web version of this article.)

varieties, the LC-MS dataset (18 columns (6 varieties X 3 replicates of samples extracts) × 838 rows (peak intensity for the detected compounds) was analyzed by PCA. Two PCA models were constructed, one on the complete run time dataset and another one on a time-reduced dataset (Madala et al., 2014). At 95% confidence limit, two principal components (PCs) were enough to explain 68% of the variance (*i.e.*, PC1 = 45% & PC2 = 23% and PC1 = 44% & PC2 = 24% for the first and second PCA models, respectively (Fig. 4)). As can be observed in the score plots (Fig. 4a & 4c), the extracts of the 6 lettuce varieties were clearly separated into different groups. These results confirmed that each variety presented a characteristic metabolite profile and the reproducibility of the extraction and the LC-MS analyses.

The examination of the score plot of the PCA on the complete run time (t_r 0–24 min) (Fig. 4a) showed that the metabolite profiles of **lr**, **lor**, **and ca** extracts (on the far-left side or negative PC1 values) were fairly distinctive and separated from the other three varieties. On the other hand, **log**, **cr**, and **lb** were clustered on the plot right side (positive PC1 values). The loading plot (Fig. 4b) revealed that mostly fatty acids and lipids were the major metabolites contributing to such discrimination, *i.e.*, primary metabolites with an accumulation that is often dependent on growth conditions (temperature, water, soil, and light,) rather than on genetic differences.

Considering that our aim was related to the distribution of the bioactive secondary metabolites, PCA was repeated on a time-reduced window (t_r 0–10.76 min), where most fatty acids and lipids were excluded from the analysis. Score and loading plots of the time-reduced PCA model (Fig. 4c & 4d) revealed a slightly different distribution of the separated varieties. Furthermore, a disaccharide and several amino acids (pyroglutamic acid, leucine, hexosyl pyroglutamic acid, and hexosyl isoleucine) were more enriched in the romaine **log** variety accounting for its palatable taste and justifying its nutritional importance. On the other hand, **cr**, **ca**, and **lb** varieties were characterized by a high abundance of tetrahydro-β-carboline-carboxylic acid while the red lettuce varieties (**lr** and **lor**) showed a clear cluster with negative PC2 values, which was attributed to high chlorogenic acid.

3.5.2. Orthogonal partial least squares-discriminant analysis (OPLS-DA)

OPLS-DA is a supervised multivariate data analysis method that is commonly applied to find the discriminant variables between two groups of samples, *e.g.*, LC-MS datasets of two categories of plant species/varieties with different physicochemical characteristics or geographical origins. This is to be achieved by categorizing all samples into the corresponding two groups so that only the discriminating signals are thought out and distinguished (Saber et al., 2021). Accordingly, the study was further extended to detect the possible impact of the leaf color on the lettuce metabolome, since leaf pigmentation is often affected by the presence of antioxidant phenolic compounds (Kim et al., 2016). An OPLS-DA model of two classes (t_r 0–10.76 min, Suppl. Fig. S27) was built with the red lettuce samples (**lor** and **lr**) and the green lettuce samples (**log**, **cr**, **ca**, and **lb**), which already showed a certain clustering in the score plots of the PCA models (Fig. 4a & 4c). The OPLS-DA model showed good fitness ($R^2_Y = 0.85$) and predictive ability ($Q^2 = 0.79$) (see the optimization and validation parameters in Suppl. Fig. (S28)).

The OPLS-DA score plot (Suppl. Fig. S27a), shows that red lettuce samples were clearly separated from green lettuce samples. The loadings S-plot compared the variable magnitude against its reliability (Suppl. Fig. S27b), where the covariance (p[1]) was plotted against the correlation (p(corr)[1]). Therefore, this graphic helped visualize the most relevant metabolites for the discrimination, which in this case were highlighted as red circles. The importance of these metabolites for the discrimination was also established using the VIP plot (Suppl. Fig. S27c). The VIP plot revealed 10 relevant metabolites for the discrimination (VIP > 2), including 1 flavonoid (kaempferol hexuronide) and 4 phenolic acids (chlorogenic, chicoric, quinic, and ferulic acids) that were enriched in **lor** and **lr** samples (Suppl. Fig. S27b) and thus can be considered as distinctive marker constituents of these varieties. This suggested a possible high antioxidant activity of these red lettuce types. It is worth noting that no carotenoids, which are well known to affect lettuce leaf pigmentation (Kim et al., 2016), were detected for the discrimination due to the polar conditions applied to prepare the lettuce extracts.

3.5.3. Correlation with antibacterial activity

PLS analysis, as a supervised approach, was applied to further investigate the association between the abundance of the annotated metabolites (Table 1) and the antibacterial activity against both *S. aureus* strains (Suppl. Table S3) of the studied lettuce extracts, with emphasis on the secondary metabolites (t_r 0–10.76 min). A PLS biplot combining score and loading plots was performed to visualize the relationship between samples and variables contributing to the separation between varieties. The LC-MS dataset of the annotated metabolites and the antibacterial activity were represented by variables X and Y, respectively. The acquired PLS biplot (Fig. 5a) showed good fitness (R^2_Y cum = 0.997) and predictive ability (Q^2 cum = 0.99), see the validation parameters in Suppl. Fig. (S29-S30). As can be observed in Fig. 5a, the antibacterial activity against both *S. aureus* strains (Y variables) was projected close to almost all lettuce varieties, suggesting that they were strongly correlated, but with **lor** samples showing less correlation. This was consistent with antibacterial study results where all varieties were active against both strains with **lor** exhibiting the least activity against the MRSA strain (Suppl. Table S3).

The correlation analysis was further extended by computing Pearson's correlation coefficient, and a correlogram was constructed (Fig. 5c) to reveal the strength of the relationship among the different variables. Nevertheless, the analysis was narrowed down by emphasizing metabolites with PLS VIP ≥ 0.7 (Azizan et al., 2020), hence 34 metabolites were selected (Fig. 5b). Correlations with p-value > 0.05 were considered non-significant and were represented by a blank white space (Fig. 5c). The color and size of the circles were proportional to the correlation coefficients (r). Positive correlations were shown in blue (different blue shades; with dark blue representing the strongest correlation), while negative correlations were in red (different red shades; with dark red representing the weakest correlation).

The obtained correlogram (Fig. 5c) showed significant correlations among metabolites **17**, **19**, **23**, **24**, **27**, **28**, **29**, **43**, **47**, **60**, **63**, **70**, **77**, **82**, **85**, & **87** and the antibacterial activity. Among these metabolites, the sesquiterpene 8-deacetylmatricarin-8-sulfate (**63**) and amino acids (hexosyl pyroglutamic acid (**17**), pyroglutamic acid derivative (**19**), hexosyl isoleucine (**23**), isoleucine derivative (**24**), hexosyl phenylalanine (**28**), and phenylalanine (**29**)) were moderately correlated with the antibacterial activity, while oxy-fatty acids (hydroxy octanedioic (**60**) and hydroxy hexadecenedioic (**82**) acids) were strongly correlated.

Sesquiterpene lactones are a major class of metabolites reported in lettuce (Ismail et al., 2019), which are attracting interest for their antimicrobial properties, probably mediated by the cyclopentenone ring moiety that has shown moderate antibacterial activity against Gram-positive bacteria (Cappiello et al., 2020). Natural amino acids and their derivatives constitute an important class of antimicrobial agents, and several known antibacterial candidates are based on amino acid scaffolds. The majority of the molecular targets for amino acid-based antibiotics are enzymes involved in the biosynthesis of peptidoglycan (*i.e.*, murein), a principal component of the bacterial cell wall (Nowak et al., 2021). Fatty acids are recognized as potential alternatives to conventional antibiotics, and various fatty acids have been reported to selectively inhibit or disrupt biofilm formation by a wide variety of bacteria, including *S.aureus* by suppressing the expression of quorum-sensing regulated genes, responsible for virulence factors (Kumar et al., 2020). The level of unsaturation and hydroxylation in the fatty acid carbon chain significantly influences membrane fluidity and antimicrobial susceptibility of microbes, and a recent study revealed that hydroxylated fatty acids presented greater antibacterial activities

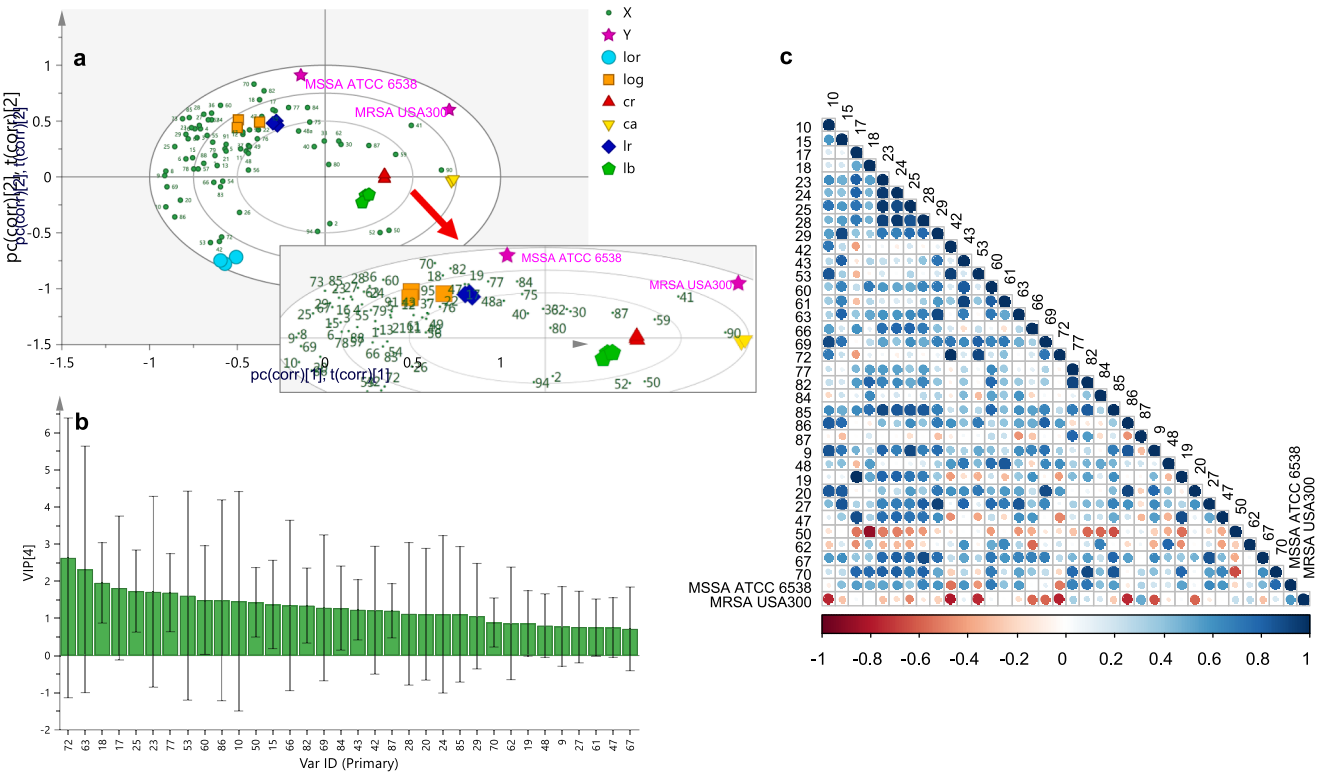

Fig. 5. (**a**) PLS score-loading biplots describing the correlations of the annotated metabolites in *L. sativa* varieties with antibacterial activity. (**b**) The resulting metabolites with variable importance to projections (VIP) values ≥ 0.7. (**c**) Correlogram visualizing the correlations of the identified metabolites (VIP ≥ 0.7) with antibacterial activity. Correlation with *p*-value > 0.05 are considered non-significant and are represented by a blank white space. Color and size of the circles are proportional to the correlation coefficients. Positive and negative correlations are shown in blue (different shades; dark blue shows the strongest correlation) and red (different shades; dark red shows the weakest correlation), respectively. See Table 1 for the metabolite names. (For interpretation of the references to color in this figure legend, the reader is referred to the web version of this article.)

against *S. aureus* when compared to their non-hydroxylated analogs (Snoch et al., 2019).

3.5.4. Correlation with antihemolytic effect

The same strategy was followed to investigate the correlation of the annotated metabolites and antihemolytic effect against both *S. aureus* strains. The biplot (Fig. 6a) constructed (t_r 0–10.76 min, R^2_Y cum = 0.99, Q^2 cum = 0.97, see the validation parameters in Suppl. Fig. (S29-S30)) revealed that the antihemolytic effect against the MSSA strain was projected close to the most active varieties (**cr**, **lr**, **lb**, and **log**), while **lor** and **ca** varieties were located close to the antihemolytic effect against MRSA confirming their improved effect against the methicillin-resistant strain, in agreement with the bioactivity results (Fig. 2). The correlogram (Fig. 6c) was performed in this case with the 32 metabolites that displayed VIP ≥ 0.7 (Fig. 6b). Six metabolites (**43**, **50**, **52**, **62**, **63**, & **84**) were found to significantly correlate with the antihemolytic effect (Fig. 6c), of which the sesquiterpene 8-deacetylmatricarin-8-sulfate (**63**), the amino acid isoleucyl-isoleucine derivative (**84**), and the alkaloids tetrahydro-β-carboline-carboxylic acid (**50**) and tetrahydro-β-carboline (**52**) exhibited the strongest correlation. The antibacterial activity of β-carboline alkaloids has been previously revealed and a recent study identified a β-carboline alkaloid dimer in *Strichnos* species, which showed a potent antibacterial activity against three multidrug-resistant clinical isolates of *S. aureus*. This study also highlighted that the presence of the tryptamine unit in the alkaloid nucleus is essential for such activity (Casciaro et al., 2019).

Based on the correlation studies, it could be generally concluded that amino acids, oxy-fatty acids, sesquiterpenes, and β-carboline alkaloids were fundamental to the antibacterial and antihemolytic activities of lettuce varieties against the *S. aureus* stains.

4. Conclusions

Six varieties of *L. sativa* leaves have been comprehensively investigated for their metabolite profiles using LC-MS/MS analysis assisted by molecular networking, allowing the annotation of 195 metabolites belonging to different classes. Multivariate data analyses (PCA and OPLS-DA) were used for clarifying the variations and determining the main metabolite markers for variety authentication and quality control. Amino acids and disaccharides were found more enriched in romaine **log** variety rationalizing its palatable taste and important nutritional value, while **cr**, **ca**, and **lb** presented a high abundance of tetrahydro-β-carboline-carboxylic acid. Furthermore, the red varieties (**lor** and **lr**) showed higher contents of chlorogenic and chicoric acids contents, suggesting their antioxidant potential. Multivariate data analysis showed that *L. sativa* varieties were differenced by both primary and secondary metabolites, which can serve as chemotaxonomic markers. However, they could be also solely discriminated according to the variety or the color considering mainly the secondary metabolites (t_r 0–10.76 min of the chromatogram), which are a more specific and diverse source of bioactives with great potential for therapeutic applications.

The antibacterial and antivirulence potential of the investigated *L. sativa* varieties against two strains of methicillin-sensitive and methicillin-resistant *S. aureus* have been assessed and validated by qPCR. All lettuce varieties showed a significant antibacterial activity against both strains. Antihemolytic effect was significant in all cases against the sensitive strain MSSA and, as expected, slightly lower for the resistant strain MRSA, with **lor** and **ca** showing the greatest effect and **cr** a non-significant effect. The observed bioactivities of the different varieties were found to be strongly correlated to their enriched phyto-constituents represented by sesquiterpenes, β-carboline alkaloids, amino

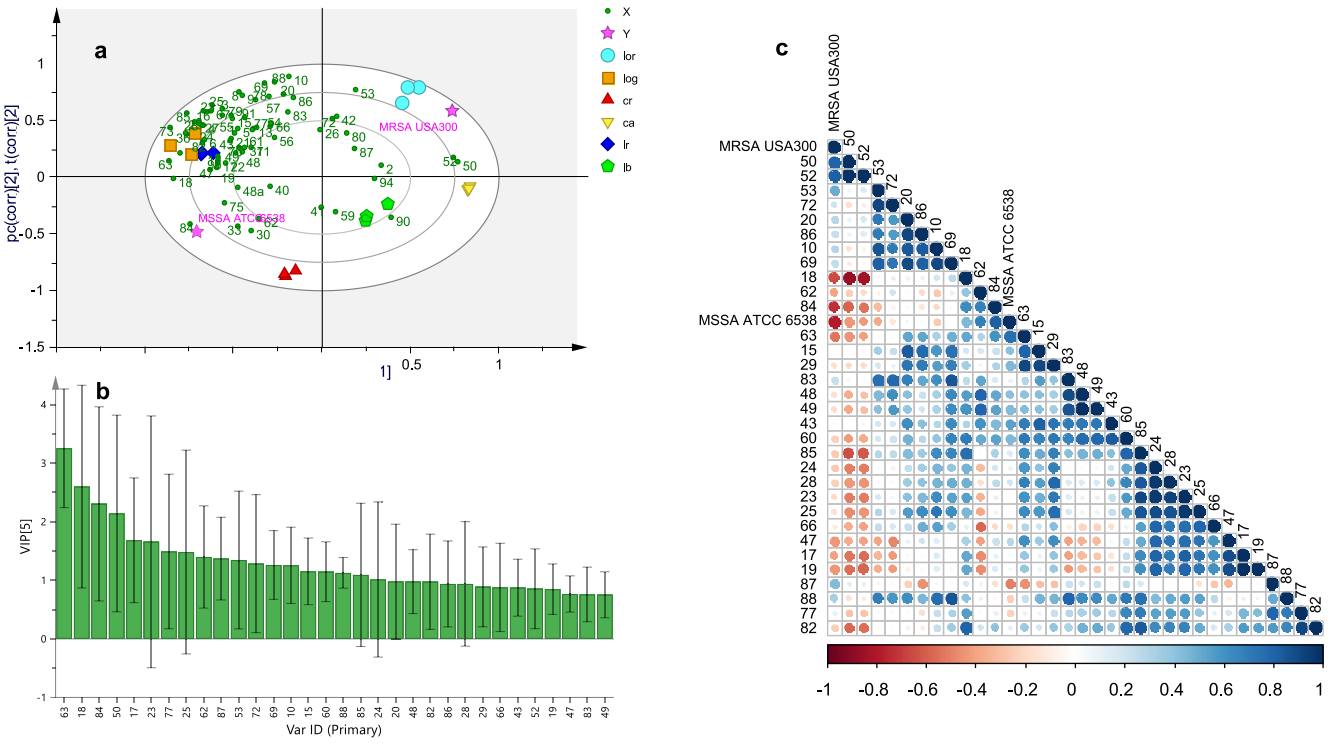

Fig. 6. (**a**) PLS score-loading biplots describing the correlations of the annotated metabolites in *L. sativa* varieties with antihemolytic effect. (**b**) The resulting metabolites with variable importance to projections (VIP) values ≥ 0.7. (**c**) Correlogram visualizing the correlations of the identified metabolites (VIP ≥ 0.7) with antihemolytic effect. Correlation with *p*-value > 0.05 are considered non-significant and are represented by a blank white space. Color and size of the circles are proportional to the correlation coefficients. Positive and negative correlations are shown in blue (different shades; dark blue shows the strongest correlation) and red (different shades; dark red shows the weakest correlation), respectively. See Table 1 for the metabolite names. (For interpretation of the references to color in this figure legend, the reader is referred to the web version of this article.)

acids, and oxy-fatty acids. Results point to lettuce varieties naturally rich in metabolites with the greatest antibacterial and antivirulence potential, which may be relevant for the development of functional foods, nutraceuticals, or novel breeding programs. However, the mechanism underlying the synergistic interactions among these metabolites must be clarified, and large-scale *in vitro* and *in vivo* experiments would be needed to establish their mammalian safety.

CRediT authorship contribution statement

Asmaa M. Otify: Conceptualization, Methodology, Investigation, Formal analysis, Validation, Data curation, Visualization, Writing – original draft. **Shahira A. ElBanna:** Conceptualization, Methodology, Investigation, Formal analysis, Validation, Data curation, Visualization, Writing – original draft. **Basma M. Eltanany:** Methodology, Formal analysis, Validation, Data curation, Writing – review & editing. **Laura Pont:** Methodology, Writing – review & editing. **Fernando Benavente:** Supervision, Writing – review & editing. **Rana M. Ibrahim:** Conceptualization, Methodology, Visualization, Writing – review & editing.

Declaration of Competing Interest

The authors declare that they have no known competing financial interests or personal relationships that could have appeared to influence the work reported in this paper.

Data availability

Data will be made available on reasonable request.

Acknowledgements

Basma M. Eltanany would like to thank the Egyptian Ministry of Higher Education for funding her *postdoctoral* research stay at the Bioanalysis group of the University of Barcelona.

Shahira A. ElBanna would like to thank Prof. Dr. Ahmed S. Attia, and Assoc. Prof. Dr. Maha M. Ismail, members of the Microbiology and Immunology Department of the Faculty of Pharmacy of Cairo University, for sharing the bacterial strains through the department library. A special gratitude to Prof. Dr. Ahmed S. Attia for providing us with the *hla* primers.

Funding source

This research did not receive any specific grant from funding agencies in the public, commercial, or not-for-profit sectors.

Appendix A. Supplementary data

Supplementary data to this article can be found online at https://doi.org/10.1016/j.foodres.2023.113178.

References

Azizan, A., Lee, A. X., Abdul Hamid, N. A., Maulidiani, M., Mediani, A., Abdul Ghafar, S. Z., … Abas, F. (2020). Potentially Bioactive Metabolites from Pineapple Waste Extracts and Their Antioxidant and α-Glucosidase Inhibitory Activities by 1H NMR. *Foods, 9*, 173. https://doi.org/10.3390/foods9020173

Byrdwell, W. C., Kubzdela, N., & Goldschmidt, R. (2021). Changes in compositions of galactolipids, triacylglycerols, and tocopherols of lettuce varieties (Lactuca sativa L.) with type, age, and light source. *Journal of Food Composition and Analysis, 100*, Article 103631. https://doi.org/10.1016/j.jfca.2020.103631

Calvano, C. D., Bianco, M., Ventura, G., Losito, I., Palmisano, F., & Cataldi, T. R. (2020). Analysis of phospholipids, lysophospholipids, and their linked fatty acyl chains in

yellow lupin seeds (*Lupinus luteus* L.) by liquid chromatography and tandem mass spectrometry. *Molecules, 25*, 805. https://doi.org/10.3390/molecules25040805
Cappiello, F., Loffredo, M. R., Del Plato, C., Cammarone, S., Casciaro, B., Quaglio, D., … Ghirga, F. (2020). The Revaluation of Plant-Derived Terpenes to Fight Antibiotic-Resistant Infections. *Antibiotics (Basel), 9*, 325. https://doi.org/10.3390/antibiotics9060325
Casciaro, B., Calcaterra, A., Cappiello, F., Mori, M., Loffredo, M. R., Ghirga, F., … Quaglio, D. (2019). Nigritanine as a New Potential Antimicrobial Alkaloid for the Treatment of Staphylococcus aureus-Induced Infections. *Toxins, 11*, 511. https://doi.org/10.3390/toxins11090511
Choi, J. S., Kim, J. Y., Woo, W. S., & Young, H. S. (1988). Isolation of a β-carboline alkaloid from the leaves ofAllium tuberosum. *Archives of Pharmacal Research, 11*, 270–272. https://doi.org/10.1007/BF02857761
Clifford, M. N., Johnston, K. L., Knight, S., & Kuhnert, N. (2003). Hierarchical scheme for LC-MSn identification of chlorogenic acids. *Journal of Agricultural and Food Chemistry, 51*, 2900–2911. https://doi.org/10.1021/jf026187q
Cosgrove, S. E., Sakoulas, G., Perencevich, E. N., Schwaber, M. J., Karchmer, A. W., & Carmeli, Y. (2003). Comparison of mortality associated with methicillin-resistant and methicillin-susceptible Staphylococcus aureus bacteremia: A meta-analysis. *Clinical Infectious Diseases, 36*, 53–59. https://doi.org/10.1086/345476
Dinges, M. M., Orwin, P. M., & Schlievert, P. M. (2000). Exotoxins of Staphylococcus aureus. *Clinical Microbiology Reviews, 13*, 16–34. https://doi.org/10.1128/cmr.13.1.16
Fahy, E., Subramaniam, S., Murphy, R. C., Nishijima, M., Raetz, C. R. H., Shimizu, T., … Dennis, E. A. (2009). Update of the LIPID MAPS comprehensive classification system for lipids. *Journal of lipid research, 50*(Suppl), S9–S14. https://doi.org/10.1194/jlr.R800095-JLR200
FAOSTAT Statistical Database. (2021). Crops and livestock products. Retrieved from Food and Agriculture Organization of the United Nations https://www.fao.org/faostat/en/#data/QCL. Accessed May 25, 2022.
Farag, M. A., Otify, A. M., El-Sayed, A. M., Michel, C. G., ElShebiney, S. A., Ehrlich, A., & Wessjohann, L. A. (2019). Sensory Metabolite Profiling in a Date Pit Based Coffee Substitute and in Response to Roasting as Analyzed via Mass Spectrometry Based Metabolomics. *Molecules, 24*, 3377. https://doi.org/10.3390/molecules24183377
Feng, J., Sun, D., Wang, L., Li, X., Guan, J., Wei, L., … Wang, B. (2021). Biochanin A as an alpha-hemolysin inhibitor for combating methicillin-resistant Staphylococcus aureus infection. *World Journal of Microbiology and Biotechnology, 38*, 6. https://doi.org/10.1007/s11274-021-03182-4
Ferreyra, M. L. F., Sebastián, P. R., & Casati, P. (2012). Flavonoids: Biosynthesis, biological functions, and biotechnological applications [Review]. *Frontiers in Plant Science, 3*. https://doi.org/10.3389/fpls.2012.00222
Fleitas Martínez, O., Cardoso, M. H., Ribeiro, S. M., & Franco, O. L. (2019). Recent Advances in Anti-virulence Therapeutic Strategies With a Focus on Dismantling Bacterial Membrane Microdomains, Toxin Neutralization, Quorum-Sensing Interference and Biofilm Inhibition. *Frontiers in Cellular and Infection Microbiology, 9*, 74. https://doi.org/10.3389/fcimb.2019.00074
German, J. B. (1999). Food Processing and Lipid Oxidation. In L. S. Jackson, M. G. Knize, & J. N. Morgan (Eds.), *Impact of Processing on Food Safety. Advances in Experimental Medicine and Biology, 459* pp. 23–50). Boston, MA: Springer. https://doi.org/10.1007/978-1-4615-4853-9_3.
Gonelimali, F. D., Lin, J., Miao, W., Xuan, J., Charles, F., Chen, M., & Hatab, S. R. (2018). Antimicrobial Properties and Mechanism of Action of Some Plant Extracts Against Food Pathogens and Spoilage Microorganisms. *Frontiers in Microbiology, 9*, 1639. https://doi.org/10.3389/fmicb.2018.01639
Grumann, D., Nübel, U., & Bröker, B. M. (2014). Staphylococcus aureus toxins–their functions and genetics. *Infection, Genetics and Evolution, 21*, 583–592. https://doi.org/10.1016/j.meegid.2013.03.013
Hung, H. C., Joshipura, K. J., Jiang, R., Hu, F. B., Hunter, D., Smith-Warner, S. A., … Willett, W. C. (2004). Fruit and vegetable intake and risk of major chronic disease. *The Journal of the National Cancer Institute, 96*, 1577–1584. https://doi.org/10.1093/jnci/djh296
Ibrahim, R. M., Eltanany, B. M., Pont, L., Benavente, F., ElBanna, S. A., & Otify, A. M. (2023). Unveiling the functional components and antivirulence activity of mustard leaves using an LC-MS/MS, molecular networking, and multivariate data analysis integrated approach. *Food Research International, 168*, Article 112742. https://doi.org/10.1016/j.foodres.2023.112742
Ismail, H., Gillespie, A. L., Calderwood, D., Iqbal, H., Gallagher, C., Chevallier, O. P., … Green, B. D. (2019). The Health Promoting Bioactivities of Lactuca sativa can be Enhanced by Genetic Modulation of Plant Secondary Metabolites. *Metabolites, 9*, 97. https://doi.org/10.3390/metabo9050097
Kenny, O., & O'Beirne, D. (2009). The effects of washing treatment on antioxidant retention in ready-to-use iceberg lettuce. *International Journal of Food Science & Technology, 44*, 1146–1156. https://doi.org/10.1111/j.1365-2621.2009.01935.x
Kim, M. J., Moon, Y., Tou, J. C., Mou, B., & Waterland, N. L. (2016). Nutritional value, bioactive compounds and health benefits of lettuce (Lactuca sativa L.). *Journal of Food Composition and Analysis, 49*, 19–34. https://doi.org/10.1016/j.jfca.2016.03.004
Köfeler, H. C., Fauland, A., Rechberger, G. N., & Trötzmüller, M. (2012). Mass spectrometry based lipidomics: An overview of technological platforms. *Metabolites, 2*, 19–38. https://doi.org/10.3390/metabo2010019
Kumar, P., Lee, J. H., Beyenal, H., & Lee, J. (2020). Fatty Acids as Antibiofilm and Antivirulence Agents. *Trends in Microbiology, 28*, 753–768. https://doi.org/10.1016/j.tim.2020.03.014
Liigand, P., Kaupmees, K., Haav, K., Liigand, J., Leito, I., Girod, M., … Kruve, A. (2017). Think Negative: Finding the best ESI/MS mode for your analyte. *Analytical Chemistry, 89*, 5665–5668. https://doi.org/10.1021/acs.analchem.7b00096
Lindqvist, K. (1960). On the origin of cultivated lettuce. *Hereditas, 46*, 319–350. https://doi.org/10.1111/j.1601-5223.1960.tb03091.x
Livak, K. J., & Schmittgen, T. D. (2001). Analysis of relative gene expression data using real-time quantitative PCR and the 2(-Delta Delta C(T)) Method. *Methods, 25*, 402–408. https://doi.org/10.1006/meth.2001.1262
Madala, N. E., Piater, L. A., Steenkamp, P. A., & Dubery, I. A. (2014). Multivariate statistical models of metabolomic data reveals different metabolite distribution patterns in isonitrosoacetophenone-elicited Nicotiana tabacum and Sorghum bicolor cells. *SpringerPlus, 3*, 254. https://doi.org/10.1186/2193-1801-3-254
Martin-Arjol, I., Bassas-Galia, M., Bermudo, E., Garcia, F., & Manresa, A. (2010). Identification of oxylipins with antifungal activity by LC-MS/MS from the supernatant of Pseudomonas 42A2. *Chemistry and Physics of Lipids, 163*, 341–346. https://doi.org/10.1016/j.chemphyslip.2010.02.003
Mukaka, M. M. (2012). Statistics corner: A guide to appropriate use of correlation coefficient in medical research. *Malawi Medical Journal, 24*, 69–71.
Nowak, M. G., Skwarecki, A. S., & Milewska, M. J. (2021). Amino Acid Based Antimicrobial Agents – Synthesis and Properties. *ChemMedChem, 16*, 3513–3544. https://doi.org/10.1002/cmdc.202100503
Otify, A. M., Ibrahim, R. M., Abib, B., Laub, A., Wessjohann, L. A., Jiang, Y., & Farag, M. A. (2023). Unveiling metabolome heterogeneity and new chemicals in 7 tomato varieties via multiplex approach of UHPLC-MS/MS, GC–MS, and UV–Vis in relation to antioxidant effects as analyzed using molecular networking and chemometrics. *Food Chemistry, 417*, Article 135866. https://doi.org/10.1016/j.foodchem.2023.135866
Pepe, G., Sommella, E., Manfra, M., De Nisco, M., Tenore, G. C., Scopa, A., … Campiglia, P. (2015). Evaluation of anti-inflammatory activity and fast UHPLC–DAD–IT-TOF profiling of polyphenolic compounds extracted from green lettuce (Lactuca sativa L.; var. Maravilla de Verano). *Food Chemistry, 167*, 153–161. https://doi.org/10.1016/j.foodchem.2014.06.105
Pink, D. A. C., & Keane, E. M. (1993). 40 - Lettuce: Lactuca sativa L. In G. Kalloo & B. O. Bergh (Eds.), *Genetic Improvement of Vegetable Crops* (pp. 543-571). Pergamon. https://doi.org/10.1016/B978-0-08-040826-2.50044-8.
Prestinaci, F., Pezzotti, P., & Pantosti, A. (2015). Antimicrobial resistance: A global multifaceted phenomenon. *Pathog Glob Health, 109*, 309–318. https://doi.org/10.1179/2047773215y.0000000030
Saber, F. R., Mohsen, E., El-Hawary, S., Eltanany, B. M., Elimam, H., Sobeh, M., & Elmotayam, A. K. (2021). Chemometric-enhanced metabolic profiling of five Pinus species using HPLC-MS/MS spectrometry: Correlation to in vitro anti-aging, anti-Alzheimer and antidiabetic activities. *Journal of Chromatography B, 1177*, Article 122759. https://doi.org/10.1016/j.jchromb.2021.122759
Saini, R. K., Prasad, P., Shang, X., & Keum, Y.-S. (2021). Advances in Lipid Extraction Methods- A Review. *International Journal of Molecular Sciences, 22*, 13643. https://doi.org/10.3390/ijms222413643
Sawada, Y., Nakabayashi, R., Yamada, Y., Suzuki, M., Sato, M., Sakata, A., … Saito, K. (2012). RIKEN tandem mass spectral database (ReSpect) for phytochemicals: A plant-specific MS/MS-based data resource and database. *Phytochemistry, 82*, 38–45. https://doi.org/10.1016/j.phytochem.2012.07.007
Schwachtje, J., Fischer, A., Erban, A., & Kopka, J. (2018). Primed primary metabolism in systemic leaves: A functional systems analysis. *Scientific Reports, 8*, 1–11. https://doi.org/10.1038/s41598-017-18397-5
Schymanski, E. L., Jeon, J., Gulde, R., Fenner, K., Ruff, M., Singer, H. P., & Hollender, J. (2014). Identifying Small Molecules via High Resolution Mass Spectrometry: Communicating Confidence. *Environmental Science & Technology, 48*, 2097–2098. https://doi.org/10.1021/es5002105
Simirgiotis, M. J., Cuevas, H., Tapia, W., & Borquez, J. (2012). Edible *Passiflora* (banana passion) fruits: A source of bioactive *C*-glycoside flavonoids obtained by HSCCC and HPLC-DAD-ESI/MS/MS. *Planta Med, 78*, 1242–1243. https://doi.org/10.1055/s-0032-1321129
Snoch, W., Stępień, K., Prajsnar, J., Staroń, J., Szaleniec, M., & Guzik, M. (2019). Influence of Chemical Modifications of Polyhydroxyalkanoate-Derived Fatty Acids on Their Antimicrobial Properties. *Catalysts, 9*(6), 510.
Thamkaew, G., Sjöholm, I., & Galindo, F. G. (2021). A review of drying methods for improving the quality of dried herbs. *Critical Reviews in Food Science and Nutrition, 61*, 1763–1786. https://doi.org/10.1080/10408398.2020.1765309
Tong, S. Y., Davis, J. S., Eichenberger, E., Holland, T. L., & Fowler, V. G., Jr. (2015). Staphylococcus aureus infections: Epidemiology, pathophysiology, clinical manifestations, and management. *Clinical Microbiology Reviews, 28*, 603–661. https://doi.org/10.1128/cmr.00134-14
Weinstein, M. P. (2018). Clinical and Laboratory Standards Institute (CLSI), Performance standards for antimicrobial susceptibility testing.
Yang, N.-Y., Yang, Y.-F., & Li, K. (2013). Analysis of Hydroxy Fatty Acids from the Pollen of Brassica campestris L. var. oleifera DC. by UPLC-MS/MS. *Journal of Pharmaceutics, 2013*, Article 874875. https://doi.org/10.1155/2013/874875